Superfluids and supersolids on frustrated two-dimensional lattices

Ganpathy Murthy*
Department of Physics and Astronomy, The Johns Hopkins University, Baltimore, Maryland 21218

Daniel Arovas
Physics Department 0319, University of California at San Diego, La Jolla, California 92093-0319

Assa Auerbach
Department of Physics, Technion IIT, Haifa, Israel
(Received 24 July 1996)

We study the ground state of hard-core bosons with nearest-neighbor hopping and nearest-neighbor interactions on the triangular and *kagomé* lattices by mapping to a system of spins ($S=1/2$), which we analyze using spin-wave theory. We find that the both lattices display superfluid and supersolid (a coexistence of superfluid and solid) order as the parameters and filling are varied. Quantum fluctuations seem large enough in the *kagomé* system to raise the interesting possibility of a disordered ground state. [S0163-1829(97)09605-7]

INTRODUCTION

A supersolid is a state of matter which simultaneously exhibits both solid and superfluid properties. That is to say, it displays both long-ranged positional order as well as finite superfluid density and, naïvely, off-diagonal long-ranged order (ODLRO). The intriguing suggestion by Andreev and Lifshitz[1] that vacancies in solid ^{4}He might Bose condense in the vicinity of the melting line has, to our knowledge, never been experimentally verified.[2,3] Nonetheless, a sizeable literature has developed on the theoretical properties of supersolids.[4–16] In two dimensions, the physics of Josephson-junction arrays[17] has also stimulated the theoretical study of supersolids. Most of the work is based on the contributions of Matsuda and Tsuneto[18] and of Liu and Fisher,[19] who established some key concepts in the theory of lattice-based supersolid models. Of central importance is the mapping between a hard-core lattice Bose gas and a spin-1/2 quantum magnet:

$$a_i^\dagger \leftrightarrow S_i^+ , \quad a_i \leftrightarrow S_i^- , \quad n_i = a_i^\dagger a_i \leftrightarrow S_i^z - \frac{1}{2} . \tag{1}$$

Thus, an occupied site is represented by an up spin, while an empty site is represented by a down spin. An interacting hard-core lattice Bose gas with nearest-neighbor hopping t, nearest-neighbor repulsion V, and chemical potential μ is thereby equivalent to the anisotropic $S=1/2$ Heisenberg model

$$\mathcal{H} = \sum_{\langle ij \rangle} \left[J_\parallel S_i^z S_j^z + J_\perp (S_i^x S_j^x + S_i^y S_j^y) \right] - H \sum_i S_i^z , \tag{2}$$

where $J_\parallel = V$ is an antiferromagnetic longitudinal exchange, $J_\perp = -2t$ is a ferromagnetic transverse exchange, and $H = \mu - (1/2) z V$ is an external magnetic field (z is the lattice coordination number). The spin model exhibits a global $U(1)$ symmetry with respect to rotations about the $\hat{z}$ axis, which of course means total particle number conservation in the boson language. The boson condensate order parameter is related to the transverse magnetization density via $\langle a_i^\dagger \rangle = \langle S_i^+ \rangle$, while the boson compressibility $K = \partial n / \partial \mu$ is the magnetic susceptibility $\chi = \partial M_z / \partial H$. Liu and Fisher identified four phases of interest: (i) a normal fluid, in which the magnetization is uniform and in the $\hat{z}$ direction, (ii) a normal solid, in which the magnetization lies along $\hat{z}$ yet is spatially modulated at some wave vector $\mathbf{k}$, (iii) a superfluid, in which the magnetization is uniform and has a component which lies in the x-y plane, and (iv) a supersolid, in which there simultaneously exists a nonzero transverse component to the magnetization $\mathbf{M}_\perp$, as well as a spatial modulation of the longitudinal magnetization M_z. (An incompressible normal fluid is also called a Mott insulator.)

If one relaxes the hard-core constraint in favor of a finite on-site repulsion U, one obtains the Bose-Hubbard model

$$\mathcal{H} = -t \sum_{\langle ij \rangle} (a_i^\dagger a_j + a_j^\dagger a_i) - \mu \sum_i n_i + \frac{1}{2} U \sum_i n_i (n_i - 1) + V \sum_{\langle ij \rangle} n_i n_j . \tag{3}$$

This model has been extensively studied since the seminal work of Fisher *et al.*,[20] who considered the model with $V=0$ in the context of a superconductor-insulator transition. A study of this model in the presence of disorder has led to an understanding of the Bose glass.[21] On a two-dimensional square lattice, and for $V \neq 0$, the model was studied at $T=0$, for both finite and infinite U, by Scalettar *et al.*,[14] Bruder, Fazio, and Schön,[6] and van Otterlo and co-workers[7,8] using mean-field theory and quantum Monte Carlo techniques. To summarize their results, no supersolid phase is observed at half filling ($\langle n \rangle = 1/2$), where a first-order transition occurs as a function of V between superfluid (small V) and a Néel solid [large V, $\mathbf{k}=(\pi,\pi)$]. (Large next-nearest-neighbor repulsion V' stabilizes a striped phase, the colinear solid.) Away from half filling, there is no normal solid phase, and the transition is instead from superfluid to supersolid. The supersolid phase exhibits both a peak in the static structure

factor $S(\mathbf{k})$ at the Néel vector (and properly proportional to the lattice volume), and a nonzero value of the superfluid density ρ_s. Again, next-nearest neighbor V' can stabilize a striped supersolid phase with anisotropic ρ_s. One can also obtain Mott insulating phases with fractional filling in the presence of next-nearest neighbor interactions.

In this paper, we will investigate the properties of the model in Eq. (2) on frustrated two-dimensional lattices. We are motivated by the fascinating interplay between frustration, quantum fluctuations, order, and disorder which has been seen in quantum magnetism.

Frustration enhances the effects of quantum fluctuations. Indeed, as early as 1973, Fazekas and Anderson[23,24] raised the possibility that for such systems, quantum fluctuations might destroy long-ranged antiferromagnetic order even at zero temperature. In many cases, frustration leads to an infinite degeneracy at the classical (or mean field) level not associated with any continuous symmetry of the Hamiltonian itself. In these cases, it is left to quantum (or thermal) fluctuations to lift this degeneracy and select a unique ground state,[25,26] sometimes with long-ranged order. Our models exhibit both a depletion (but not unambiguous destruction) of order due to quantum fluctuations, as well as the phenomenon of ''order by disorder.''

In our work, we will choose the units of energy to be $J_\parallel$, writing $\Delta \equiv t/V = J_\perp/2J_\parallel$, and $h \equiv H/J_\parallel$. We will be following closely the analysis of the anisotropic triangular lattice antiferromagnet by Kleine, Müller-Hartmann, Frahm, and Fazekas (KMFF),[27] who performed a mean-field ($S=\infty$ limit) and spin-wave theory (order $1/S$ corrections to mean-field) analysis. Contemporaneously with KMFF, Chubukov and Golosov[28] derived the spin-wave expansion for an isotropic Heisenberg antiferromagnet in a magnetic field, while Sheng and Henley[29] obtained the spin-wave theory for the anisotropic antiferromagnet in the absence of a field.

The mean-field phase diagram is shown in Fig. 1 (both the triangular and *kagomé* lattices have the same mean-field phase diagram up to a rescaling of h). Notice that the supersolid phase appears in a broad region of Δ and filling. The reason the supersolid is so robust is that the lattice frustrates a full condensation into a solid. Generically, frustrated lattices might be good places to look for this phase.

Let us briefly concentrate on $h=0$ before describing the entire phase diagram. We will be assuming a three sublattice structure throughout. The mean-field state is then described by three polar and three azimuthal angles: $(\theta_A, \theta_B, \theta_C, \phi_A, \phi_B, \phi_C)$, and is invariant under uniform rotation of the azimuths.

Due to the ferromagnetic coupling in the x-y spin directions the mean-field solution is always coplanar. Just as in KMFF, there is a one-parameter family of degenerate mean-field solutions in the zero-field case (originally found by Miyashita and Kawamura[30]). The A sublattice polar angle θ_A may be chosen as the free parameter; spin-wave theory (SWT) is necessary to lift the degeneracy and uncover the true ground state. Figure 2 shows the ground-state energy in SWT as a function of θ_A for the triangular lattice at $\Delta=0.25$. Using SWT we also compute the fluctuations of the spins, and the consequent quantum-corrected magnetization and the solid and ODLRO order parameters. Figure 3 illustrates these quantities in mean field and to leading order in SWT

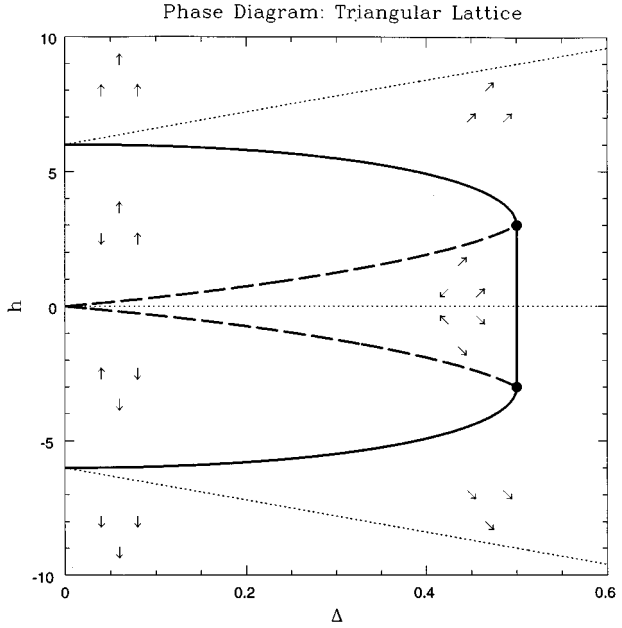

FIG. 1. Mean-field phase diagram for the triangular lattice. The *kagomé* lattice phase diagram differs only by a rescaling of h. Heavy lines denote first-order transitions, light lines second-order transitions, and dashed lines denote linear instabilities.

(where S has been set equal to 1/2) as a function of Δ for the triangular lattice. It is clear that the quantum corrected S^z is very close to zero for all Δ, reflecting the fact that at $h=0$ the lattice is half-filled. Two sublattices acquire large corrections due to quantum fluctuations (even in the Ising limit $\Delta \to 0$), while the third has only small quantum corrections. This is very similar to the fully antiferromagnetic case studied by KMFF. Therefore, even at $S=1/2$ the solid order survives. The off-diagonal order parameter S^x is reduced in

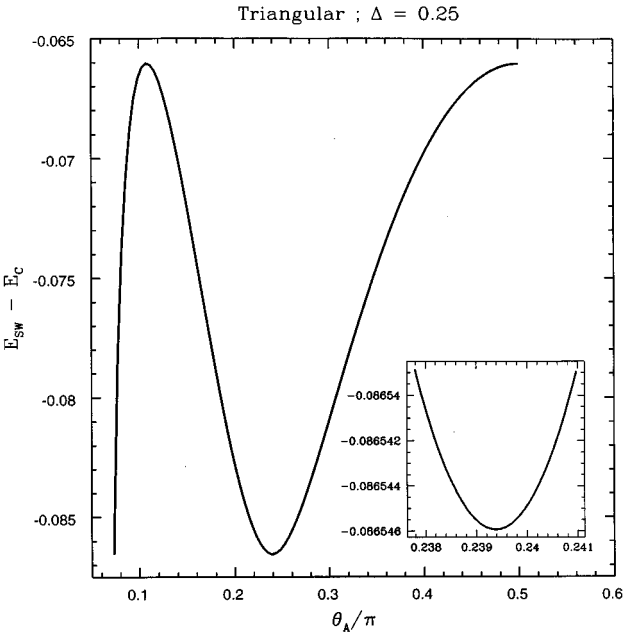

FIG. 2. Ground-state energy of the triangular lattice at $\Delta=0.25$ as a function of θ_A. The minimum is quadratic.

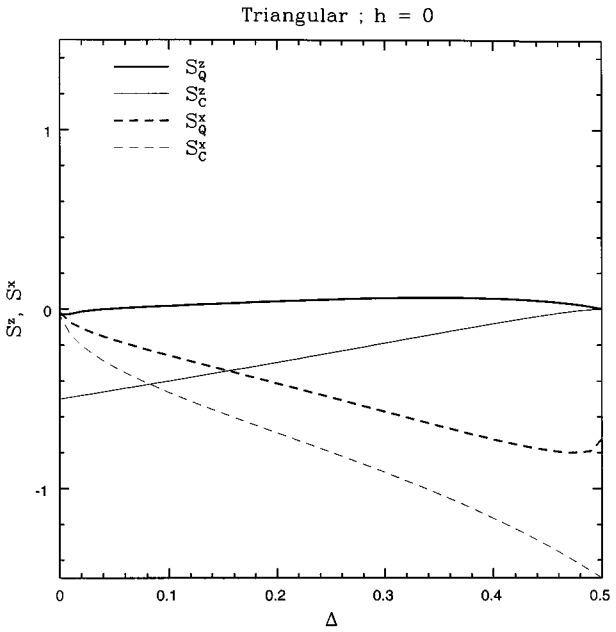

FIG. 3. Classical and quantum magnetizations for the triangular lattice, S_z and S_x per site, as a function of Δ at the true ground state. The full quantum-corrected S_z is always close to zero, while the quantum-corrected S_x is always nonzero.

magnitude by quantum corrections, but goes to zero only as $\Delta \to 0$. Supersolid order survives quantum fluctuations for the triangular lattice, at least in this order of SWT.

Let us now consider the *kagomé* lattice. There is a qualitative difference between the antiferro-ferromagnetic case considered here, $\Delta \geqslant 0$, and the fully antiferromagnetic case $\Delta \leqslant 0$, which has been exhaustively explored for the Heisenberg limit $\Delta = -1$ (for a partial set of references, see Refs. 31–38). For the fully antiferromagnetic case there are local motions of the spins that move the system on the degeneracy submanifold, leading to a much larger ground-state degeneracy for the *kagomé* lattice than for the triangular lattice. However, for $\Delta \geqslant 0$, the ferromagnetic transverse interaction eliminates the possibility of these local motions, resulting in a ground-state degeneracy parametrized only by θ_A, just as in the triangular lattice.

We carried out SWT for the two long-range ordered configurations shown in Fig. 4—a three sublattice ''$\mathbf{q}=0$'' state, and a nine sublattice $\sqrt{3}\times\sqrt{3}$ structure,[35,36] respectively. These states have the same mean-field ground-state energy. It will turn out that two of the three sublattices have the same spin orientation in the ground state for both lattices. With this proviso, note that the $\mathbf{q}=0$ structure has one twofold axis and a mirror plane (point group C_{2v}), while the $\sqrt{3}\times\sqrt{3}$ structure has a sixfold axis and a mirror plane (point group C_{6v}). Once again SWT selects the true ground state. When quantum fluctuations are accounted for, we find that the $\sqrt{3}\times\sqrt{3}$ structure always has lower energy than the $\mathbf{q}=0$ structure, to the numerical accuracy of our calculations. More importantly, the fluctuations of the spins on six of the nine sublattices diverge in the limit $h \to 0$, as shown in Fig. 5. This divergence is the consequence of a flat (dispersionless) mode at zero energy as $h \to 0$. Higher-order terms in the spin wave expansion will lift this mode and remove the divergence.[25,39] However, the fluctuations remain large for $S = 1/2$, as we estimate in Sec. III. This indicates that quantum fluctuations may be strong enough to wash out any order, including ODLRO, on two of the sublattices, which raises the intriguing possibility of a partially disordered ground state at $T = 0$. It must be emphasized that we have not demonstrated that

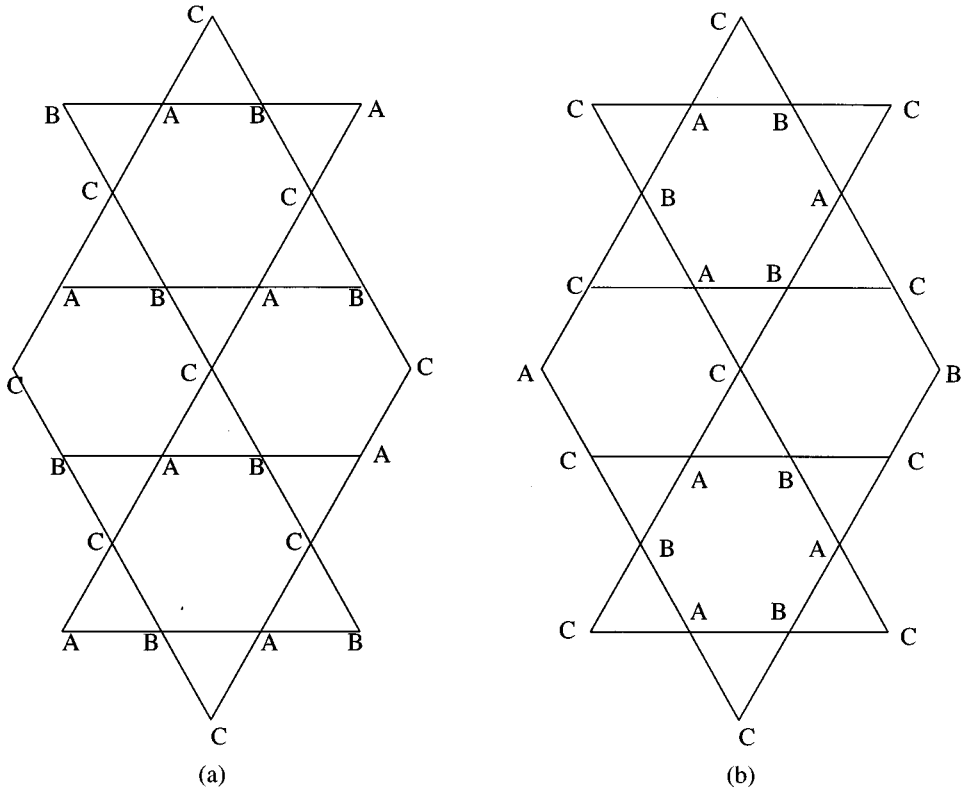

FIG. 4. The two long-range-ordered structures on the *kagomé* lattice. (a) the $q=0$ structure and (b) the $R3$ structure.

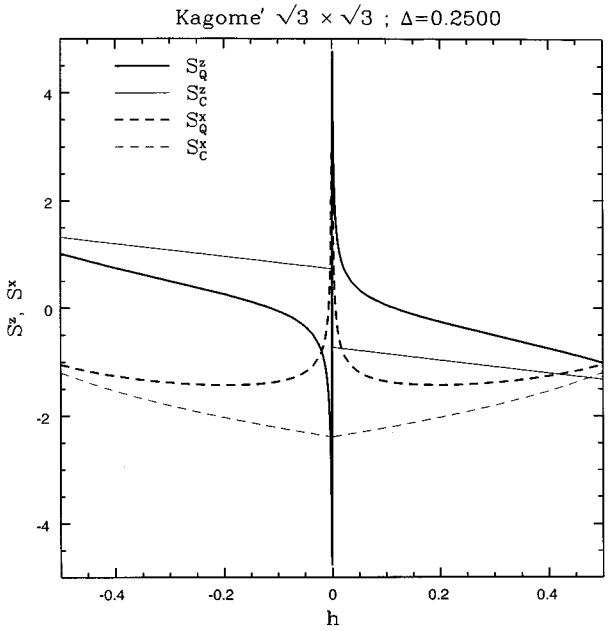

FIG. 5. Classical and quantum-corrected values of the magnetizations S_z and S_x per site as a function of h at $\Delta=0.25$ for the $R3$ structure on the *kagomé* lattice. Notice the divergence as $h\to 0$. This is an artifact of SWT.

this is so: the fluctuations could be correlated between different sites, there could be long-range order with a larger unit cell, a condensed array of vortices, etc. This problem merits further study, with, e.g., quantum Monte Carlo methods.

Let us now turn to a fuller description of Fig. 1, where four types of mean-field states are present (solid lines indicate first-order transitions). We adopt the nomenclature of Ref. 14 (see Fig. 12 of this reference for comparison). At high fields h the system is in a Mott phase—incompressible and fully polarized. As the field is lowered, for any $\Delta>0$, the system enters a compressible superfluid phase (SF), with $\theta_A=\theta_B=\theta_C>0$. A first-order transition from the superfluid to an incompressible Néel solid (NS) at filling fraction 2/3 [magnetization per site $M_z=\pm(1/3)S$] occurs for $\Delta<1/2$. Finally, the supersolid phase (SS) exists for $\Delta<1/2$ between the two symmetry-related Néel solid lobes. There is a tricritical point at $(\Delta^*,h^*)=[(1/2),3]$. Quantum fluctuations will modify these mean-field phase boundaries. Since the superfluid state, we have found, benefits the most from spin-wave energy corrections, it will encroach on its neighbors as S decreases from ∞. Increasing h tends to suppress quantum fluctuations.

We will present each of the above results in more detail in the rest of this paper. Section I concentrates on the mean-field theory and the mean-field phase diagram. Section II describes the selection of the true ground state by quantum fluctuations at $h=0$, and the form of the spin-wave excitations for arbitrary h. Section III presents the suppression of order by quantum fluctuations. We end with our conclusions, connections to experimental work, and open questions.

I. MEAN-FIELD THEORY

The mean-field limit is obtained by setting $S=\infty$. Formally, we first generalize the model from $S=1/2$ to a model with a spin-S at each site. We then represent each spin as a classical vector of magnitude S, $S^\alpha=S\Omega^\alpha$, where $\hat{\Omega}$ is a unit vector in three dimensions. We rescale the magnetic field by S and write

$$\mathcal{H}_{\rm MF}/S^2=\sum_{\langle ij\rangle}\Omega_i^z\Omega_j^z-\Delta\sum_{\langle ij\rangle}(\Omega_i^x\Omega_j^x+\Omega_i^y\Omega_j^y)-h\sum_i\Omega_i^z. \tag{4}$$

In the mean-field solution, all spins lie in the x-z plane. Furthermore, it turns out that the triangular and both *kagomé* structures have the same mean-field energy, to within a constant factor (up to a separate rescaling of h in the case of the *kagomé* structures), so we will consider all three cases simultaneously. Note that coplanar states have been selected at the mean-field level for the *kagomé* lattice, in contrast to the fully antiferromagnetic case.

A. Zero field

Consider first mean-field ground states on the triangular and *kagomé* lattices that have a three-sublattice structure. The three specific cases are the usual sublattice structure on the triangular lattice, the $\mathbf{q}=0$ structure on the *kagomé* lattice, and the $\sqrt{3}\times\sqrt{3}$ structure on the *kagomé* lattice. The nine sublattices of the $\sqrt{3}\times\sqrt{3}$ structure are organized into three groups (A,B,C) of three, so that an A site has two B and two C neighbors. Thus, the energy per site, in units of S^2, is

$$\begin{aligned}e_{\rm MF}&\equiv E_{\rm MF}/NS^2\\&=(\cos\theta_A\cos\theta_B+\cos\theta_B\cos\theta_C+\cos\theta_C\cos\theta_A)\\&\quad-\Delta(\sin\theta_A\sin_B+\sin\theta_B\sin\theta_C+\sin\theta_C\sin\theta_A)\end{aligned} \tag{5}$$

on the triangular lattice and $z_{\rm Kag}/z_{\rm Tri}=2/3$ this value on the *kagomé* lattice.

Miyashita and Kawamura[30] have shown that there is a one-parameter family of degenerate ground states for this classical problem for arbitrary Δ, which does not seem to be related to any obvious symmetry of the model. Following KMFF, and writing $\beta_i=\theta_i-(\theta_A+\theta_B+\theta_C)$, and defining the two-dimensional vectors $\boldsymbol{\mu}_i=(\sin\beta_i,\cos\beta_i)$, we can write the mean-field energy in terms of the two-component vector $\boldsymbol{\mu}\equiv\boldsymbol{\mu}_A+\boldsymbol{\mu}_B+\boldsymbol{\mu}_C$:

$$e_{\rm MF}=\frac{1}{4}(1-\Delta)(\boldsymbol{\mu}^2-3)+\frac{1}{2}(1+\Delta)\mu_y. \tag{6}$$

Therefore $e_{\rm MF}$, while nominally depending on the three angles θ_i, actually depends only on two combinations of them, leaving one parameter free. We can then parametrize the degenerate ground states by θ_A, by defining $\theta_B=\epsilon-\delta$, and $\theta_C=\epsilon+\delta$, where

$$\tan\epsilon=-\frac{\tan\theta_A}{\Delta}, \tag{7}$$

$$\cos\epsilon=\frac{-\Delta\cos\theta_A}{\sqrt{1-(1-\Delta^2)\cos^2\theta_A}},$$

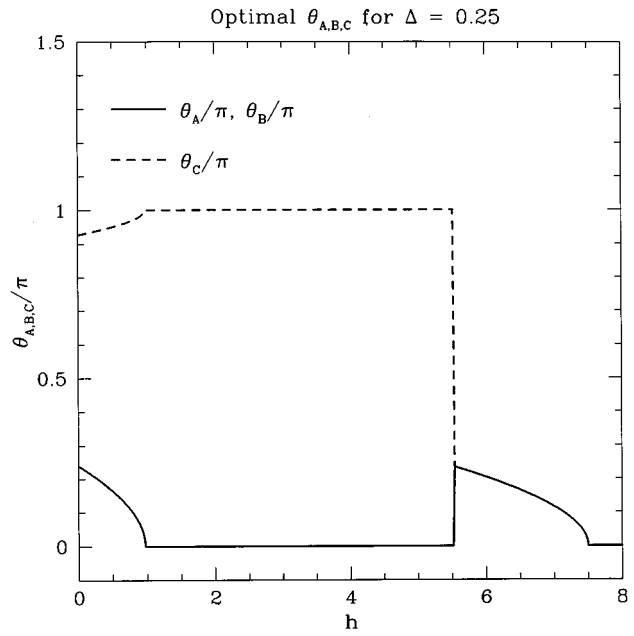

FIG. 6. Optimal $\theta_A=\theta_B$ and θ_C as a function of h for $\Delta=0.25$. Note the continuous approach to collinearity at the supersolid-solid transition, and the discontinuous change of the angles at the solid-superfluid transition.

$$\cos\delta=\frac{\Delta}{(1-\Delta)\sqrt{1-(1-\Delta^2)\cos^2\theta_A}}.$$

It is easy to verify that θ_A can lie in the range

$$\cos^{-1}\left(\frac{1}{1-\Delta}\sqrt{\frac{1-2\Delta}{1-\Delta^2}}\right)\leqslant\theta_A\leqslant\frac{1}{2}\pi.$$

As Δ increases from zero, the range of possible θ_A is compressed, and the differences $|\theta_B-\theta_A|$, $|\theta_C-\theta_A|$ shrink, until at $\Delta=1/2$ the ground state is colinear with $\theta_A=\theta_B=\theta_C=(1/2)\pi$—a featureless superfluid. For $\Delta<1/2$, in the case of zero field, the true ground state will be selected by quantum fluctuations. Minimizing $e_{\rm MF}$ gives $\mu_x=(\Delta+1)/(\Delta-1)$, $\mu_y=0$, and

$$e_{\rm MF}=-\left(\frac{1-\Delta+\Delta^2}{1-\Delta}\right). \tag{8}$$

B. Nonzero field

Turning on a field h adds an energy

$$\Delta e_{\rm MF}=-\frac{1}{3}h(\cos\theta_A+\cos\theta_B+\cos\theta_C) \tag{9}$$

per site and lifts the degeneracy described in the previous subsection, producing a unique mean-field ground state (unlike in the Heisenberg antiferromagnet[28]). We find that minimization generally leads to a state where (without loss of generality) $\theta_A=\theta_B\neq\theta_C$ in the supersolid phase. The results are plotted in Fig. 6. A rescaling of the field for the *kagomé* lattice $[h_{\rm Kag}=(2/3)h_{\rm Tri}]$ makes the entire mean-field phase diagram identical, and we have therefore shown only the triangular lattice results.

The phase diagram has already been shown in Fig. 1. Let us keep at a particular value of Δ and turn up the field h. At zero field there are two regimes, the superfluid with no solid order for $\Delta>1/2$, and the supersolid with both solid and ODLRO $(T=0)$ for $\Delta<1/2$. For $\Delta>1/2$, the ground state remains a uniform superfluid, though M_z becomes nonzero, as h is increased. The spins cant at an angle $\theta=\cos^{-1}[h/6(1+\Delta)]$. The energy in this phase is

$$e_{\rm MF}^{\rm [SF]}=-3\Delta-\frac{h^2}{12(1+\Delta)}. \tag{10}$$

Eventually, for $h>6(1+\Delta)$, every site has the maximum possible S^z, and the system is in the Mott insulator (MI) phase, with each site fully occupied with one boson. Borrowing from spin-wave results derived in Sec. II, the linear instability of the SF phase occurs at

$$h_{i1}=6\sqrt{(1+\Delta)(1-2\Delta)}. \tag{11}$$

Next focus on a specific $\Delta<1/2$, and increase the field h from zero. At zero field, the one-parameter degeneracy of the mean-field ground states has to be lifted by quantum fluctuations, which select a particular θ_A. However, it turns out that we can recover this θ_A by considering nonzero h and taking the limit $h\to0$, which gives

$$\cos^2\theta_A=\frac{1-2\Delta}{1-\Delta^2}. \tag{12}$$

It seems surprising that the ground state selected by quantum fluctuations can be predicted by an entirely classical calculation. A plausible (though nonrigorous) argument will be provided for this in terms of spin-wave theory in the next section.

As h is increased from zero, θ_A and θ_C change (recall $\theta_A=\theta_B$ throughout). At a certain critical field $h_{c1}(\Delta)$, $\mathbf{S}_C$ points exactly along the $-\hat{z}$ direction $(\theta_C=\pi)$, while $\mathbf{S}_{A,B}$ point along the $\hat{z}$ direction $(\theta_A=\theta_B=0)$. This critical field h_{c1} can be analytically determined by the following consideration: the point $\theta_A=0$, $\theta_C=\pi$ is always a stationary point of the mean-field energy. However, for $h<h_{c1}$ it is a saddle point, while for $h>h_{c1}$ it is a minimum. Therefore the second derivative matrix of $e_{\rm MF}(\theta_A,\theta_C)$ should have a zero eigenvalue at $h=h_{c1}$. Setting the determinant to zero gives

$$h_{c1}(\Delta)=\frac{3}{2}(2+\Delta-\sqrt{4-4\Delta-7\Delta^2}). \tag{13}$$

For $h<h_{c1}(\Delta)$, we are in the supersolid phase. Just above h_{c1}, however, the system is exactly 2/3 filled, and its magnetic susceptibility is zero (the compressibility of the corresponding boson system is zero). There is no superfluid order and the system is again a Mott insulator, the Néel solid. It will be seen in Sec. III that the exact filling of 2/3 survives quantum fluctuations. Since the superfluid order goes continuously to zero below the transition, it is clear that this transition is second-order within in mean-field theory. The energy of the Néel solid phase is

$$e_{\rm MF}^{\rm [NS]}=-1-\frac{h}{3}. \tag{14}$$

One can furthermore determine that the Néel solid phase is linearly stable for $3/2(2+\Delta-\sqrt{4-4\Delta-7\Delta^2}) \leq h \leq 3/2(2+\Delta+\sqrt{4-4\Delta-7\Delta^2})$.

Further increasing h, we find a critical field

$$h_{c2}(\Delta)=2(1+\Delta)+4\sqrt{(1+\Delta)(1-2\Delta)}, \tag{15}$$

beyond which the canted superfluid becomes energetically favored. The transition is first order since it is far from any linear instabilities. Finally, a second-order line at $h>h_{c3}(\Delta)=6(1+\Delta)$, signals the boundary between superfluid and fully polarized Mott phases.

When $\Delta=1/2$, we can solve analytically to find

$$\cos\theta_A=\frac{1}{3}h,$$

$$\cos\theta_C=-\frac{1}{3}h, \tag{16}$$

$$e_{\mathrm{MF}}^{[\mathrm{SS}]}=-\frac{3}{2}-\frac{1}{18}h^2.$$

This is exactly the same as the energy of the SF phase at $\Delta=1/2$ [which is characterized by all the angles satisfying $\cos\theta=(1/9)h$], which marks this vertical line as a first-order line. Note the tricritical point at $\Delta=1/2$, $h=3$, where two first-order lines (with infinite slope) meet a second-order line (with finite slope).

The situation is completely symmetric with respect to the sign of h, with the Néel solid phase now existing at 1/3 filling for $h<0$. At the mean-field level, the Δ axis is a first-order transition line up to $\Delta=1/2$, since S^z is discontinuous across it. However, for $S=1/2$ it apparently becomes continuous, at least for the triangular lattice.

The phase diagram has some similarities to the classic picture of the Mott lobes surrounded by superfluid described by Fisher, Weichman, Grinstein, and Fisher (FWGF).[20] However, there are important differences. FWGF considered local Hubbard repulsion, whereas our extended Bose-Hubbard model we consider affords the possibility of incompressible Mott phases at fillings 0, 1/3, 2/3, and 1. The Néel solid phase found by Scalettar *et al.*, for example, exists at filling 1/2. Fractional fillings have also been observed in the square lattice with frustrating longer range interactions in Ref. 6. Also, the transitions from the fractional filling MI phases to the (canted) superfluid are first order. Finally, and most notably, the entire region between the two fractional Mott lobes is taken over by the supersolid, and the supersolid gives way to the superfluid only beyond a hopping $t>(1/2)V$.

II. SPIN-WAVE THEORY

We now develop the spin-wave theory (SWT) for this problem. If $h\neq 0$, there is a unique ground state (up to permutations of the sublattices). When $h=0$, the ground-state manifold is parametrized by θ_A, and the other angles, θ_B and θ_C (in general not equal), can be determined from θ_A and Δ using Eq. (7). We implement SWT in the usual way: by first performing local rotations of the spins so that the mean-field directions point along the local z axis. Since all the spins are assumed to lie on the x-z plane, we can do this by a rotation about the y axis. Labeling the local frame spins with a tilde, we have

$$\begin{aligned} S^x_{\mathbf{R}\nu}&=\cos\theta_\nu \widetilde{S}^x_{\mathbf{R}\nu}+\sin\theta_\nu \widetilde{S}^z_{\mathbf{R}\nu},\\ S^y_{\mathbf{R}\nu}&=\widetilde{S}^y_{\mathbf{R}\nu},\\ S^z_{\mathbf{R}\nu}&=-\sin\theta_\nu \widetilde{S}^x_{\mathbf{R}\nu}+\cos\theta_\nu \widetilde{S}^z_{\mathbf{R}\nu}, \end{aligned} \tag{17}$$

where the subscript $\mathbf{R}$ labels a Bravais lattice site, ν a basis element, and θ_ν is $\theta_{A,B,C}$ depending on the mean-field orientation of the ν sublattice. The triangular lattice and the $\mathbf{q}=0$ structure on the *kagomé* lattice have three sublattices, while the $\sqrt{3}\times\sqrt{3}$ structure on the *kagomé* lattice has nine.

We now describe the spin operators in terms of Holstein-Primakoff bosons

$$\begin{aligned} \widetilde{S}^+_{\mathbf{R}\nu}&=\psi^\dagger_{\mathbf{R}\nu}\sqrt{2S-\psi^\dagger_{\mathbf{R}\nu}\psi_{\mathbf{R}\nu}}=\sqrt{2S}\,\psi^\dagger_{\mathbf{R}\nu}+\mathcal{O}(S^{-1/2}),\\ \widetilde{S}^-_{\mathbf{R}\nu}&=\sqrt{2S-\psi^\dagger_{\mathbf{R}\nu}\psi_{\mathbf{R}\nu}}\,\psi^\dagger_{\mathbf{R}\nu}=\sqrt{2S}\,\psi_{\mathbf{R}\nu}+\mathcal{O}(S^{-1/2}),\\ \widetilde{S}^z_{\mathbf{R}\nu}&=\psi^\dagger_{\mathbf{R}\nu}\psi_{\mathbf{R}\nu}-S. \end{aligned} \tag{18}$$

The Hamiltonian (restoring h for generality) is now written in Fourier space as

$$\mathcal{H}_{\mathrm{sw}}=E_0+(1/2)S\sum_{\mathbf{k}}{:}\Psi^\dagger(\mathbf{k})\begin{pmatrix} M & N\\ N & M\end{pmatrix}\Psi(\mathbf{k}){:}+\mathcal{O}(S^0) \tag{19}$$

(note the normal ordering) where the energy E_0 is given by

$$E_0=(N/K)S^2\left[\frac{1}{2}\sum_{\nu\nu'} z_{\nu\nu'}X_{\nu\nu'}-\sum_\nu h_\nu\right]. \tag{20}$$

Here, N is the total number of lattice sites, K is the number of sublattices, and we define the quantities

$$\begin{aligned} X_{\nu\nu'}&=\cos\theta_\nu\cos\theta_{\nu'}-\Delta\,\sin\theta_\nu\sin\theta_{\nu'},\\ Y_{\nu\nu'}&=\sin\theta_\nu\sin\theta_{\nu'}-\Delta\,\cos\theta_\nu\cos\theta_{\nu'},\\ h_\nu&=h\,\cos\theta_\nu, \end{aligned} \tag{21}$$

and $z_{\nu\nu'}$ is the number of ν' sublattice neighbors each ν sublattice site has. The vector $\mathbf{k}$ lives in the first Brillouin zone of the reciprocal lattice, and

$$\begin{aligned} \Psi^\dagger(\mathbf{k})=[&\psi^\dagger_1(\mathbf{k}),\psi^\dagger_2(\mathbf{k}),\ldots,\psi^\dagger_K(\mathbf{k}),\\ &\psi_1(-\mathbf{k}),\psi_2(-\mathbf{k}),\ldots,\psi_K(-\mathbf{k})]. \end{aligned} \tag{22}$$

The matrices M and N have diagonal and off-diagonal elements given by

$$M_{\nu\nu}(\mathbf{k})=h_\nu-\sum_{\nu'} z_{\nu\nu'}X_{\nu\nu'}, \tag{23}$$

$$M_{\nu\nu'}(\mathbf{k})=\frac{1}{2}(Y_{\nu\nu'}-\Delta)f_{\nu\nu'}(\mathbf{k}),$$

$$N_{\nu\nu}(\mathbf{k})=0,$$

$$N_{\nu\nu'}(\mathbf{k}) = \frac{1}{2}\,(Y_{\nu\nu'} + \Delta) f_{\nu\nu'}(\mathbf{k}),$$

where the function $f_{\nu\nu'}(\mathbf{k})$ is given by the following sum:

$$f_{\nu\nu'}(\mathbf{k}) = \sum_{\boldsymbol{\delta}}{}' \;\; \exp(i\mathbf{k}\cdot\boldsymbol{\delta}), \tag{24}$$

where the prime on the sum indicates that the sum is over nearest-neighbor vectors connecting a ν sublattice site to a ν' sublattice site.

Now we perform a Bogoliubov transformation, which amounts to finding a rank $2K$ matrix T satisfying $T^{\dagger}\Lambda T = \Lambda$, with

$$\Lambda = \begin{pmatrix} 1_{K\times K} & 0_{K\times K} \\ 0_{K\times K} & -1_{K\times K} \end{pmatrix}, \tag{25}$$

as well as $\Lambda T^{-1}\Lambda \mathcal{H}_{\mathrm{sw}} T = \omega$, a non-negative diagonal matrix with identical upper left and lower right blocks. The $\omega_{\nu}(\mathbf{k})$ are the spin-wave frequencies. The spin-wave correction to the ground-state energy is given by

$$\Delta E = \frac{1}{2}\, S \sum_{\mathbf{k}} \sum_{\nu=1}^{K} [\,\omega_{\nu}(\mathbf{k}) - M_{\nu\nu}(\mathbf{k})]. \tag{26}$$

A. Ground-state selection

Figure 2 shows the ground-state energy, including spin-wave corrections, for the triangular lattice at $h=0$ as a function of θ_A. Since the classical energy is independent of θ_A all the variation comes from the SW correction. It is clear that there are two possible values of θ_A which minimize the ground-state energy, one of them lying at the edge of the allowed range of θ_A. However, the two minima turn out to be physically identical, and correspond to a relabeling of the sublattices. We call the minimizing value of θ_A which lies away from the edge of its allowed range θ_A^{*}.

The value of θ_A^{*} can be determined by purely classical arguments, by extremizing the value of $S^z \propto \theta_A + \theta_B + \theta_C$ along the degeneracy submanifold. We have checked that this is so by a comparison of the analytic expression $\theta_A^{*} = \cos^{-1}\sqrt{(1-2\Delta)/(1-\Delta^2)}$ with the ground-state energy curves obtained from SWT. We now provide an argument indicating why this might be the case.

Our argument will be the following: For a generic θ_A there is only one mode of zero energy at $\mathbf{k}=0$, whereas if $\partial S_z/\partial\theta_A = 0$ there are two zero modes (to spin-wave order). The ground-state energy is the sum of the energies of all the modes, and does not depend on just the zero modes. However, we think it plausible that having more modes of zero energy at $\mathbf{k}=0$ drags down the energies of all the $\mathbf{k}$ modes, thus reducing the full ground-state energy. Of course this argument is not rigorous,[40] and there may be counterexamples that we are not aware of.

Let us go on to show the first statement about the number of modes of zero energy. We only sketch the argument here: We treat the issue with more generality and greater detail in the Appendix. It is helpful to think in terms of the coherent states path integral[22]

$$\mathcal{Z} = \int D[\theta_A, \theta_B, \theta_C, \phi_A, \phi_B, \phi_C] e^{-\mathcal{A}},$$
$$\mathcal{A} = \int d\tau \left(\sum_{\mathbf{r}} iS\, \cos\theta(\mathbf{r},\tau)\, \frac{\partial}{\partial\tau}\, \phi(\mathbf{r},\tau) + \mathcal{H}[\theta,\phi] \right), \tag{27}$$

where $\mathcal{H}$ stands for the spin Hamiltonian of Eq. (4) written in terms of θ and ϕ. The first term is the Berry phase contribution to the path integral, which also makes $S\cos\theta$ the momentum canonically conjugate to ϕ.

Let us concentrate on just the $\mathbf{k}=0$ modes. There are three ϕ variables and three conjugate θ variables. We choose to call one of the ϕ variables ϕ_0 corresponding to an overall rotation of all the spins around the z axis, and call the remaining ϕs, ϕ_1, and ϕ_2.

Choose any particular ground state labeled by θ_A. The Hamiltonian for small deviations from the ground-state configuration is now given by

$$\mathcal{H} = \frac{1}{2}\, \theta^T M_{\theta} \theta + \frac{1}{2}\, \phi^T M_{\phi} \phi, \tag{28}$$

where $\theta^T = (\delta\theta_A, \delta\theta_B, \delta\theta_C)$ and $\phi^T = (\phi_0, \phi_1, \phi_2)$. The first row and column of M_{ϕ} are zero since ϕ_0 does not appear in the Hamiltonian.

The general procedure for finding the normal modes is the following:

(i) Diagonalize the 2×2 block of M_{ϕ} and rescale the resulting eigenvectors so that the rescaled M'_{ϕ} becomes a unit matrix in the 2×2 block. Call the rescaled ϕ variables $\psi_{\pm}$.

(ii) Use the Berry's phase terms to identify the canonically conjugate momenta to ϕ_0, $\psi_{\pm}$ as P_0, $P_{\pm}$, respectively.

(iii) Re-express the matrix M_{θ} as a matrix M_P.

(iv) Since ϕ_0 is cyclic, its canonically conjugate momentum P_0 is conserved. Treat P_0 as a constant and form linear combinations $P'_{\pm} = P_{\pm} + \alpha_{\pm} P_0$ such that the off-diagonal terms containing P_0 are eliminated. A diagonal term multiplying P_0^2 remains.

(v) Now diagonalize the lower 2×2 block of M_P. The two eigenvalues of M_P are the squares of the energies of the normal modes of the Hamiltonian. The third normal mode corresponds to a uniform rotation of all the spins around the z axis coupled to a change in S_z, and its energy is always zero regardless of the coefficient of P_0^2.

The above is true even if there is no ground-state degeneracy. If there is ground-state degeneracy in the θ subspace the matrix M_P has a null eigenvector v_0. For generic θ_A, P_0 has nonzero overlap with v_0. In this case the above procedure always produces a zero coefficient for P_0^2. Thus there is still only one mode of zero energy, the S_z mode. Another way of seeing this is to recognize that as long as P_0 and v_0 have nonzero overlap, one can always rescale v_0 so that it becomes canonically conjugate to ϕ_0. One then has to modify $\psi_{\pm}$ to keep them independent of v_0 in the Poisson bracket sense.

However, if P_0 and v_0 have zero overlap, the null vector must lie in the subspace of $P_{\pm}$. This means one of the eigenvalues of the lower 2×2 block of M_P must be zero, implying that there is *another* zero mode of the Hamiltonian, apart from the S_z mode. The condition for P_0 and v_0 to have

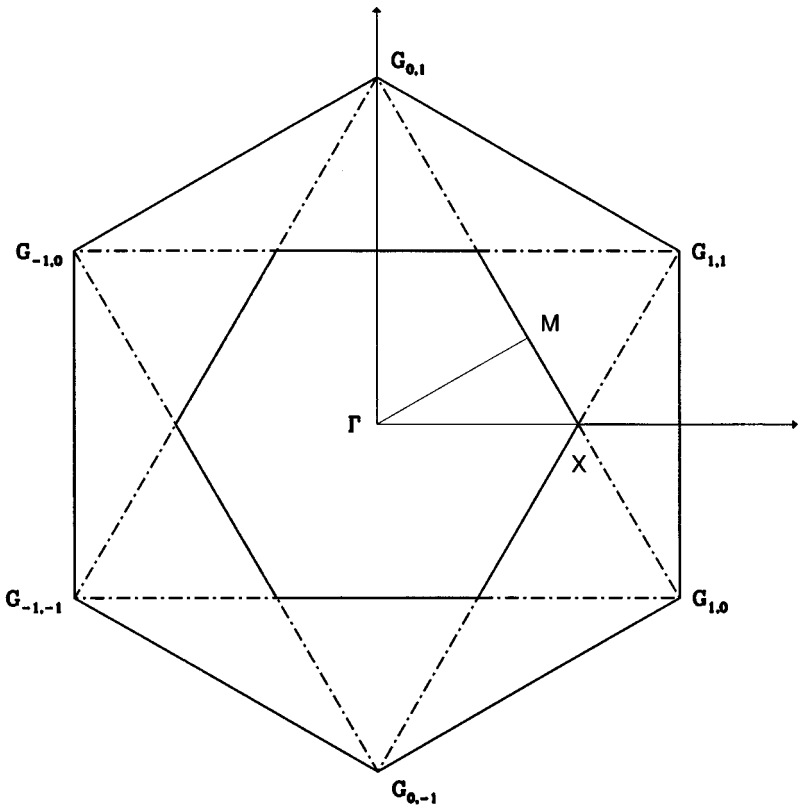

FIG. 7. The Brillouin zone of the triangular lattice and the reduced zone for the sublattice structure.

zero overlap is identical to $\partial S_z/\partial\theta_A=0$ along the degeneracy direction, which is the same as extremizing S_z.

In brief, if $\partial S_z/\partial\theta_A\neq 0$, there is only one zero mode, whereas if $\partial S_z/\partial\theta_A=0$, there are two zero modes at $\mathbf{k}=0$. A rigorous derivation is supplied in the Appendix.

We have done explicit calculations to verify all these statements for the triangular lattice. If one computes the frequencies of the $\mathbf{k}=0$ modes at a nonoptimal θ_A, one finds one mode of zero energy (the S^z mode), and two modes of nonzero energy, neither of which is exactly along the degeneracy direction. However, at precisely the optimal points, there appear *two* modes with zero energy, one of which is the S^z mode and the other exactly the degeneracy mode. The third mode still has nonzero energy.

In particular, the argument makes no assumptions about the interactions other than that they should conserve total S^z. So this result should hold even for site dilution or longer range interactions. Of course, for site dilution, one should focus on a particular realization of randomness and look at S^z over the degeneracy subspace. In general, our argument is that *the search for the true ground state can be restricted to the points on the degeneracy submanifold where all conserved quantities commute in the Poisson bracket sense with the generators of motion along the degeneracy submanifold*.

This criterion can fail if the $\mathbf{k}\neq 0$ modes do not follow the behavior of the $\mathbf{k}=0$ modes. Also, if there are more conserved quantities than degeneracy directions, not all of them may be extremized at the true ground state.

With θ_A and θ_B taking on the value quoted above, we find that θ_c is at the extreme edge of its allowed range:

$$\cos\theta_c^*=-\frac{1}{1-\Delta}\sqrt{\frac{1-2\Delta}{1-\Delta^2}}. \tag{29}$$

B. Spin-wave dispersions

1. Triangular lattice

The Brillouin zone (BZ) of the triangular lattice is shown in Fig. 7, with the lattice and reciprocal-lattice vectors being

$$\begin{aligned}\mathbf{e}_1&=a(1,0),\\ \mathbf{e}_2&=a\left(\frac{1}{2},\frac{\sqrt{3}}{2}\right),\\ \mathbf{G}_1&=\frac{4\pi}{a\sqrt{3}}\left(\frac{\sqrt{3}}{2},-\frac{1}{2}\right),\\ \mathbf{G}_2&=\frac{4\pi}{a\sqrt{3}}(0,1),\end{aligned} \tag{30}$$

where a is the lattice spacing.

As usual, we first concentrate on $h=0$. Figure 8 shows the spin-wave dispersion for $\Delta>1/2$. Since there is only one sublattice, there is only one mode. However, plotting it on the reduced BZ of the sublattice problem forces us to fold it back and represent it as three modes. In this scheme, there is one gapless mode, which is the Goldstone mode corresponding to the density fluctuations of the bosons. However, as Δ approaches 1/2, a ''roton'' minimum develops, precisely at the wave vectors corresponding to the sublattice structure, as demonstrated in Fig. 9. At exactly $\Delta=1/2$, this becomes a gapless mode, heralding the transition to the supersolid phase.

Now consider the dispersion at $h=0$ in the SS phase, which is shown in Fig. 10. There are two gapless modes

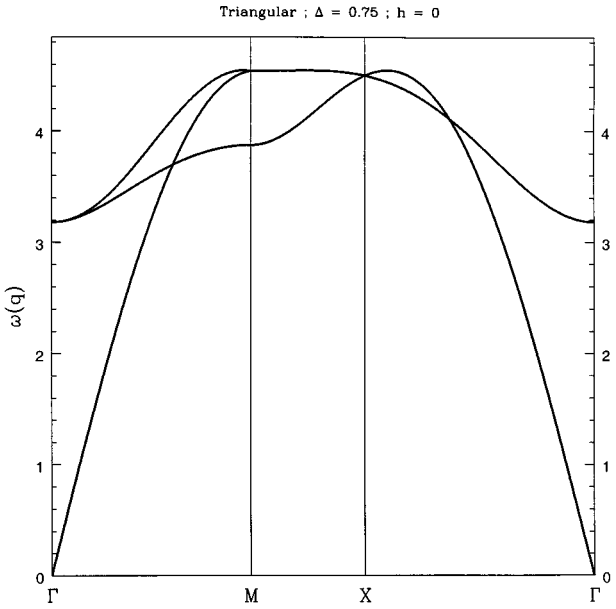

FIG. 8. Triangular lattice SW dispersion for $\Delta=0.75$, $h=0$.

within SWT. One is the standard density fluctuation, whereas the other corresponds to the degeneracy mode. The degeneracy mode will be shown to acquire a gap to higher order in $1/S$ in the next subsection.[25,39] There is a third ''optical'' mode to complete the count of the sublattice degrees of freedom. The energy scale of the two low-lying modes is Δ, while the optical mode has an energy scale of 1. As we move towards $\Delta=0$ the two low-lying modes get softer, until they become completely flat at $\Delta=0$.

However, when we turn on a field the degeneracy mode becomes gapped, as shown in Fig. 11. Let us now investigate the modes at nonzero field in the other phases, in particular

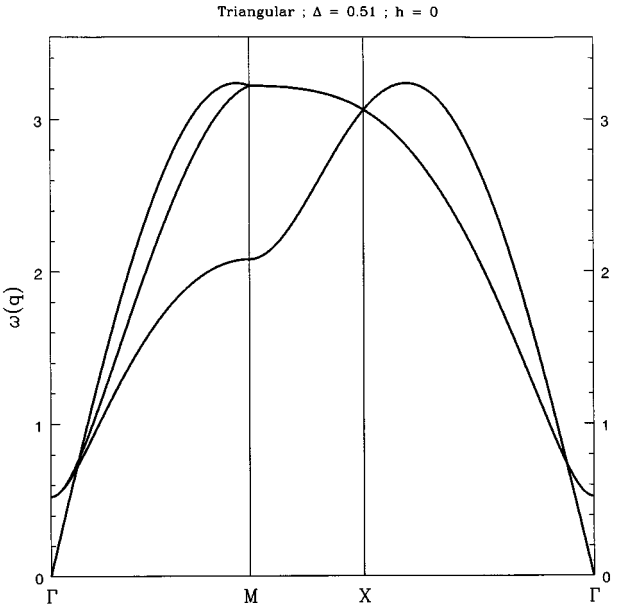

FIG. 9. Triangular lattice SW dispersion for $\Delta=0.51$, $h=0$. Note the quadratic minimum which is nearly gapless. This is the linear instability that leads to the SS phase.

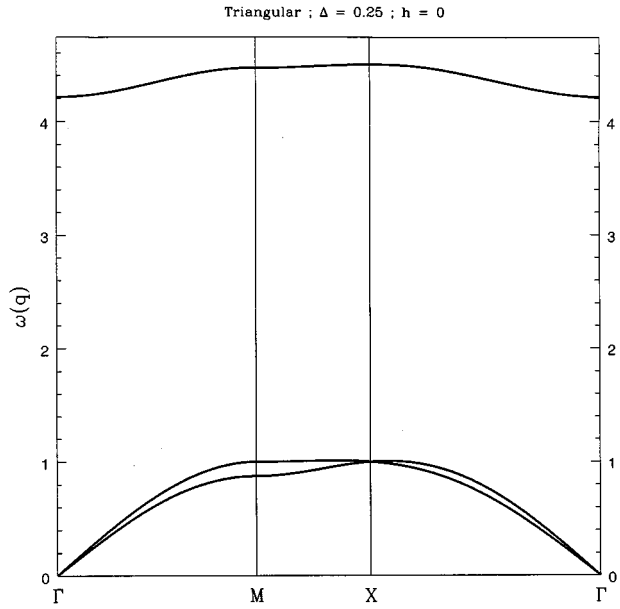

FIG. 10. Triangular lattice SW dispersion in the SS phase at $\Delta=0.25$, $h=0$.

at the transitions. The SWT for the canted spin phase can be analyzed analytically, since there is only one sublattice. We find that the SW dispersion is

$$\omega(\mathbf{k})=zS\sqrt{\Delta(1-\gamma_{\mathbf{k}})\left[\Delta+\left(1-\frac{h^2}{36(1+\Delta)}\right)\gamma_{\mathbf{k}}\right]},$$
$$\gamma_{\mathbf{k}}=\frac{1}{z}\sum_{\boldsymbol{\delta}}{}' e^{-i\mathbf{k}\cdot\boldsymbol{\delta}}, \tag{31}$$

where $z=6$ for the triangular lattice, and the prime on the sum restricts $\boldsymbol{\delta}$ to nearest-neighbor vectors. We show an example for $\Delta=0.25$, $h=6.0$ in Fig. 12. We have $-1/2\leqslant\gamma_{\mathbf{k}}\leqslant 1$,

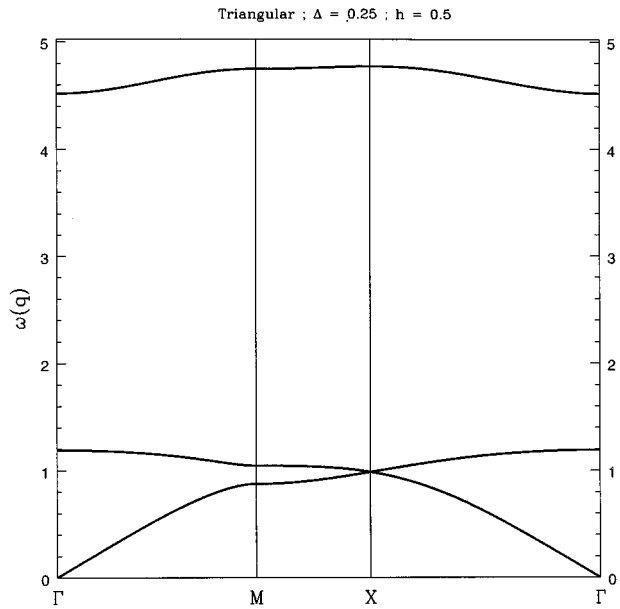

FIG. 11. Triangular lattice SW dispersion in the SS phase at $\Delta=0.25$, $h=0.5$. The degeneracy mode has become gapped.

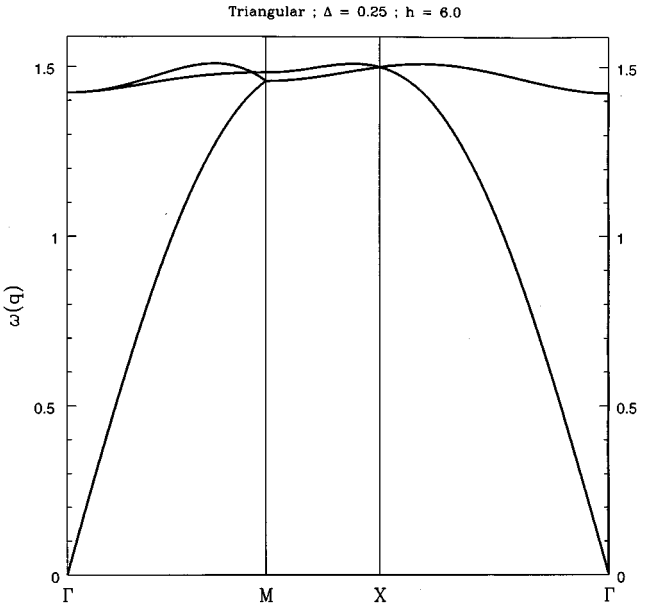

FIG. 12. Triangular lattice SW dispersion in the canted spin (CS) phase at $\Delta=0.25$, $h=6.0$. Note the single gapless density mode.

which leads to the linear instability of the SF phase, which is denoted h_{i1} in Eq. (11). Note that the mean-field energies of the various phases lead to first-order instabilities which make the linear instability irrelevant except at $\Delta=0$ and $\Delta=1/2$.

We next turn to the transition line between the supersolid and Néel solid phases, denoted by $h_{c1}(\Delta)$, a second-order line. Figure 13 shows the SW dispersion at the transition for $\Delta=0.25$, $h=0.9738$. The soft density mode is now at $\mathbf{k}=0$ and has a quadratic dispersion instead of the usual linear one. As we increase h and enter the Néel solid phase, the density mode becomes gapped, as Fig. 14 shows. The total energy

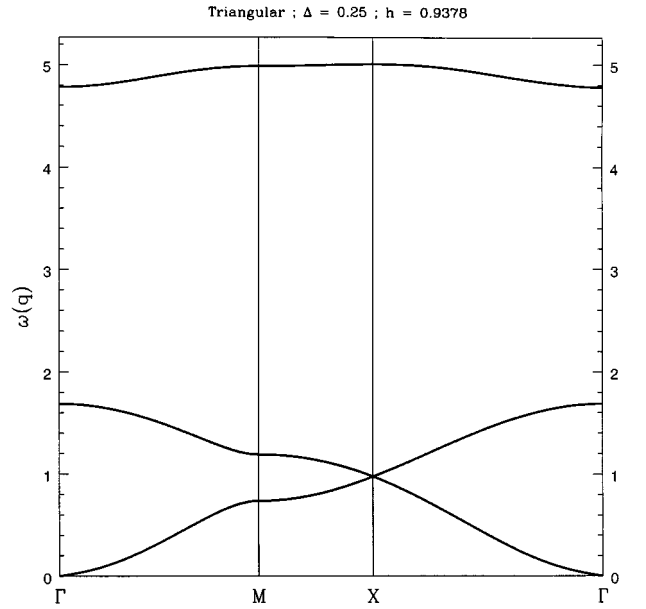

FIG. 13. Triangular lattice SW dispersion at the SS-MI transition at $\Delta=0.25$, $h=0.9738$. Note the quadratic dispersion of the gapless density mode.

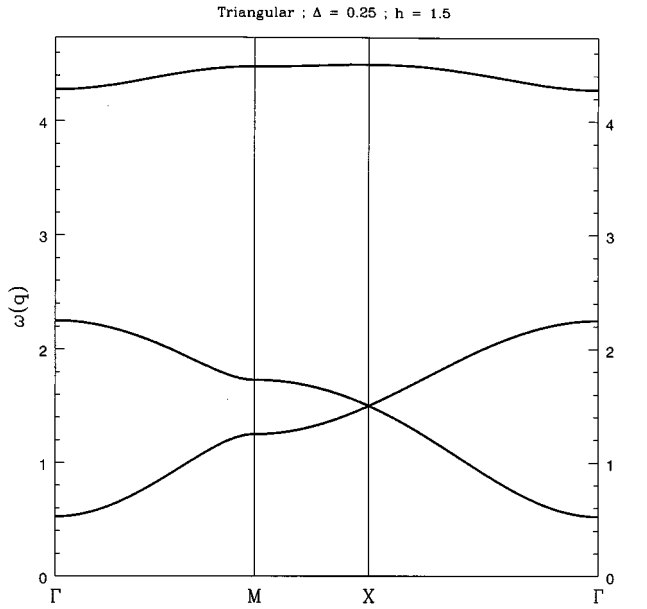

FIG. 14. Triangular lattice SW dispersion in the MI phase at $\Delta=0.25$, $h=1.5$.

(including spin-wave corrections) in the Néel solid phase is independent of h, which demonstrates its incompressibility, and hence the exact filling of 2/3 throughout this phase.

2. kagomé lattice q=0

The *kagomé* lattice is a triangular Bravais lattice with a three element basis. If a is the nearest-neighbor separation, then the Bravais lattice constant is $\tilde{a}=2a$. The spin-wave theory dispersions are quite similar to those of the triangular lattice, with the modes being softer (because of the lower coordination). Note that while the Bravais lattice is triangular, the symmetry is reduced (to C_{2v}) and the dispersion curves do not have zero slope at the zone edge (the X point). Figures 15, 16, and 17 show the dispersions in the superfluid, the supersolid, the Néel solid state, respectively. A noteworthy feature is the presence of a zero-energy mode at $h=0$ along the ΓM direction in the supersolid phase. This mode disperses and has nonzero energy except along the ΓM direction.

3. kagomé 9 sublattice structure

The $\sqrt{3}\times\sqrt{3}$ structure on the *kagomé* lattice is described by a triangular Bravais lattice of lattice constant $\tilde{a}=2\sqrt{3}a$ with a nine element basis. The elementary lattice vectors are shown in Fig. 4. The spin-wave dispersions are unremarkable except for a flat mode whose energy vanishes as $\sqrt{h}$ in the small h limit. This is connected to the degeneracy mode, which is local up to harmonic order, and will be discussed in the next subsection. All the other features are quite similar to those of the triangular lattice as shown in Figs. 18, 19, and 20.

C. Gap of the degeneracy mode

The degeneracy mode appears gapless in SWT (and in fact appears flat in the $\sqrt{3}\times\sqrt{3}$ structure on the *kagomé* lattice), but acquires a gap to higher order in the SW

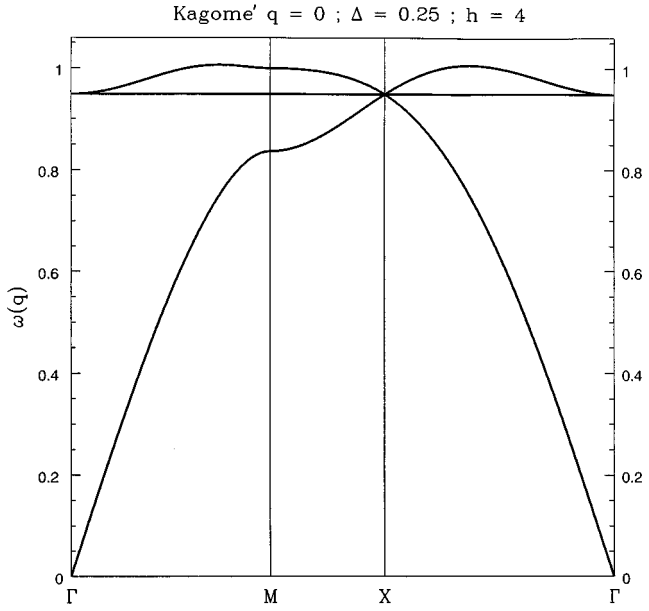

FIG. 15. *kagomé* $\mathbf{q}=0$ SW dispersion in the CS phase at $\Delta=0.25$, $h=4$.

expansion.[25,39] We will first treat the triangular lattice, and go on to the case of the *kagomé* lattice.

1. Triangular lattice

Let us concentrate on the $\mathbf{k}=0$ degeneracy mode of the triangular lattice. The easiest way to derive the gap is in the spin coherent-state path-integral language[22] introduced in the previous section.

Now imagine separating the path integral by first integrating all the modes except the $\mathbf{k}=0$ degeneracy mode (call the angles θ_A^0 and ϕ^0).

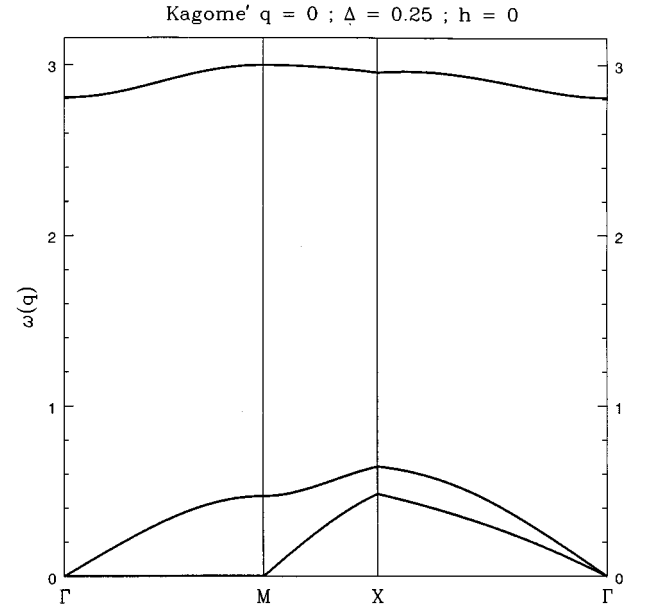

FIG. 16. *kagomé* $\mathbf{q}=0$ SW dispersion in the SS phase at $\Delta=0.25$, $h=0$. Note the flat character of the mode along the ΓM direction.

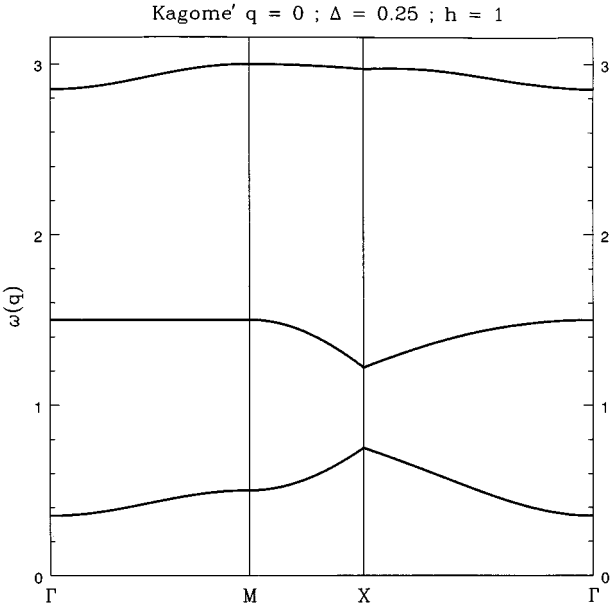

FIG. 17. *kagomé* $\mathbf{q}=0$ SW dispersion in the MI phase at $\Delta=0.25$, $h=1$.

$$\mathcal{Z}=\int D\theta_A^0 D\phi^0 \times\exp-\int d\tau\left(iS\cos\theta_A^0\frac{\partial\phi^0}{\partial\tau}+\frac{1}{2}S^2K(\phi^0)^2\right)\times\int\prod_{\mathbf{k}\neq 0}D[\theta_{\mathbf{k}},\phi_{\mathbf{k}}]e^{-\mathcal{A}'[\theta,\phi]}, \tag{32}$$

where $\mathcal{A}'$ does not include the explicitly written terms involving ϕ_0 in the preceding factor. Since the classical ground-state energy does not depend on θ_A^0, only the Berry phase term and a ''potential'' energy for ϕ^0 appear there

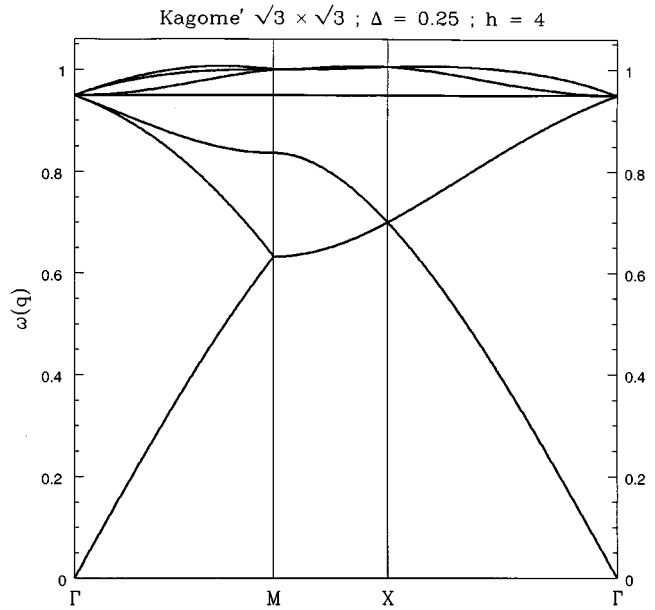

FIG. 18. *kagomé* $R3$ SW dispersion in the CS phase at $\Delta=0.25$, $h=4$.

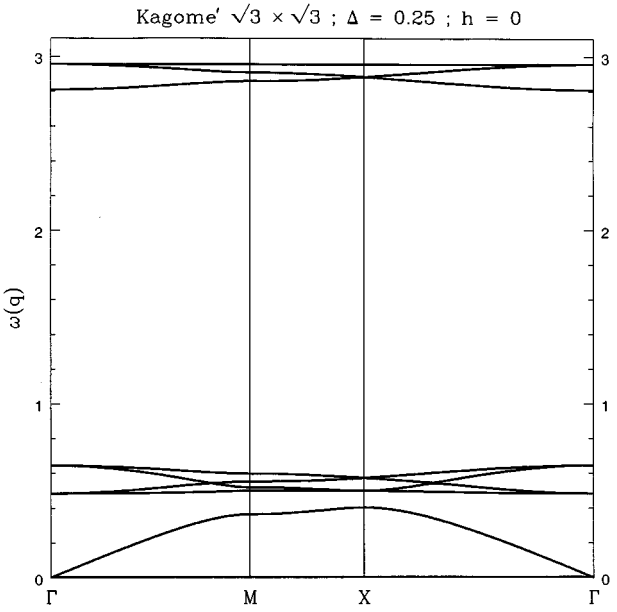

FIG. 19. *kagomé* $R3$ SW dispersion in the SS phase at $\Delta=0.25$, $h=0$. Note the completely flat zero-energy mode.

(expanded to lowest leading order). If one neglects the integration over the remainder of the modes, the degeneracy mode appears to have a potential energy but no kinetic energy. This is analogous to a particle of infinite mass, and from the simple harmonic oscillator formula $\omega=\sqrt{K/M}$, the oscillator energy is zero. This is why the mode appears gapless.

However, as seen from Fig. 2, the integration over the rest of the modes (to leading order in the spin-wave expansion) creates an effective potential which has a dependence on θ_A^0, rendering the mass M finite and the mode gapped. Since the effective potential is produced by SWT, it will be of order S, as opposed to the order S^2 potentials generated classically for the other modes. Thus the gap is order $\sqrt{S}$, compared to the energies of order S seen in SWT.

Now for the specific details. We concentrate on the neighborhood of θ_A^*, the optimal value of θ_A^0, and write $\theta_A^0=\theta_A^*+\delta\theta_A$. It is easy to see that the ϕ^0 that couples to this is $\phi^0=\phi_A(\mathbf{k}=0)-\phi_B(\mathbf{k}=0)$. The eigenvector corresponding to this mode is $(\phi_A,\phi_B,\phi_C)=[(1/2)\phi^0,-(1/2)\phi^0,0]$. For the triangular lattice the classical ''potential'' energy of a ϕ^0 deformation yields

$$K=3\Delta\,\sin^2\theta_A^*\left(1+\frac{\sin\theta_B^*}{2\sin\theta_A^*}\right). \tag{33}$$

Choosing the particular value $\Delta=0.25$ for illustration, we fit the curve in Fig. 2 near its minimum to obtain the term in the effective action $(1/2)SC(\delta\theta_A)^2$, for which we obtain $C\simeq 6$. Of course, a ''potential'' term will also be generated by the integration of the rest of the modes, but since it is order S, it can be neglected compared to the order S^2 term already present classically. We will choose the ''coordinate'' as $Q=S\,\sin\theta_A^*\phi^0$. The Berry phase term now looks like $S\,\sin\theta_A^*\delta\theta_A(\partial\phi^0/\partial\tau)$, which enables us to identify $P\equiv\delta\theta_A$ as the conjugate momentum. We now write the action as

$$S=\int d\tau\left(iP\,\frac{\partial Q}{\partial\tau}+\frac{1}{2}\,SCP^2+\frac{1}{2}\,\tilde{K}Q^2\right), \tag{34}$$

where $\tilde{K}=3\Delta[1+(1/2)(\sin\theta_C^*/\sin\theta_A^*)]$. We can now find the gap as the harmonic frequency of this oscillator:

$$\omega_0=\sqrt{SC\tilde{K}}. \tag{35}$$

The numerical value is $\omega_0\approx 2.3\sqrt{S}$. The *kagomé* lattice structure introduces new considerations, which we now address.

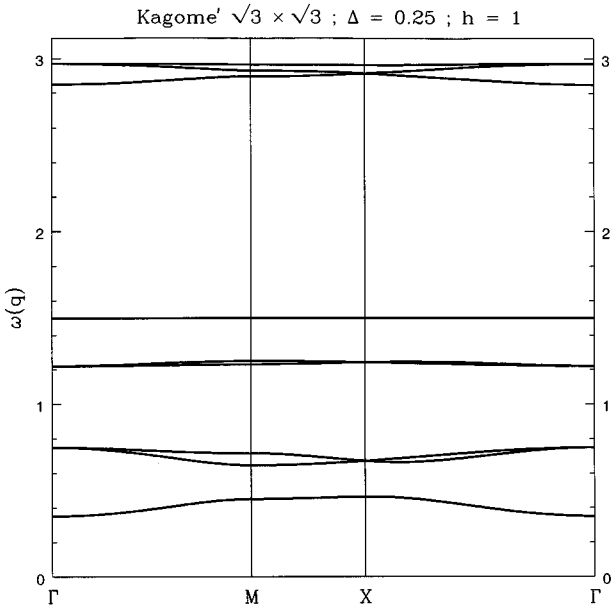

FIG. 20. *kagomé* $R3$ SW dispersion in the MI phase at $\Delta=0.25$, $h=1$.

2. kagomé lattice

The important difference that occurs for the *kagomé* lattice is that the effective action for the θ_A has a linear cusp at the minimum instead of a quadratic minimum, as shown in Figs. 21 and 22 for the $\mathbf{q}=0$ and $\sqrt{3}\times\sqrt{3}$ structures, respectively. This kind of minimum has previously been seen for the *kagomé* lattice in the fully antiferromagnetic Heisenberg case.[41,42] We assume that the degeneracy mode is nondispersing, which, at spin-wave order, is approximately true for the $\mathbf{q}=0$ structure, and exactly true for the $\sqrt{3}\times\sqrt{3}$ structure. This implies that the modes are local, and we assume this to be true even after quantum fluctuations have lifted them from zero energy. We can now interchange the roles of θ and ϕ as P and Q and consider the quantum mechanics of the Hamiltonian

$$\frac{P^2}{2M}+\lambda|Q|, \tag{36}$$

where λ is of order S. This leads to a gap in the degeneracy mode of order $S^{2/3}$. A lifting of the degeneracy mode of order $S^{2/3}$ has previously been seen in Refs. 43 and 44 in the Heisenberg case.

Since the *kagomé* $\sqrt{3}\times\sqrt{3}$ structure is always lower in energy, we will concentrate on it in the following, leaving a

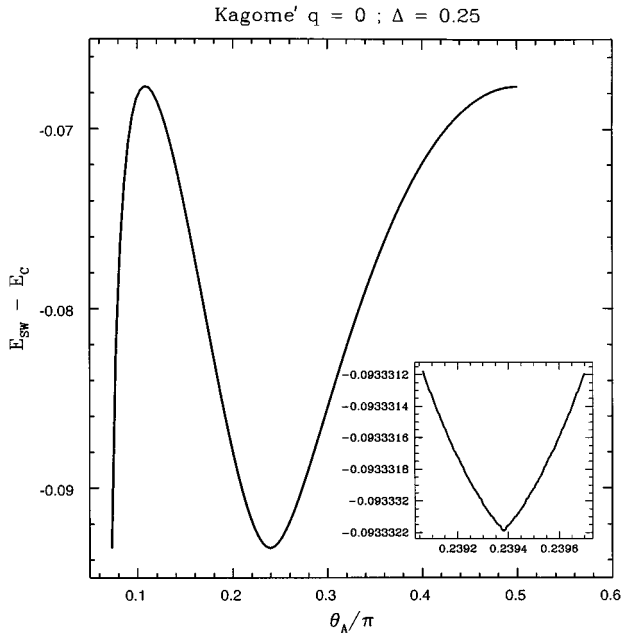

FIG. 21. Quantum energy correction versus θ_A for the *kagomé* $\mathbf{q}=0$ structure. Note the cusp at the minimum.

detailed analysis of the $\mathbf{q}=0$ structure to a future publication. The degeneracy mode which was merely gapless at $\mathbf{k}=0$ on the triangular lattice, but of nonzero energy at every other $\mathbf{k}$, becomes completely flat at zero energy on the *kagomé* lattice with the $\sqrt{3}\times\sqrt{3}$ structure. The reason is fairly straightforward. Consider an *ABABAB* hexagon in Fig. 4(b), isolated from the rest of the lattice by a ring of *C* sites. For the optimal angles it is easy to deduce that if $\theta_A=\theta_A^*+\delta\theta$, then $\theta_B=\theta_A^*-\delta\theta$ and that θ_C changes only to order $\delta\theta^2$. Any coupling between the $\delta\theta_A(\mathbf{r})$ of neighboring *ABABAB* hexagons must be mediated by the bordering θ_C, and must therefore be third order or higher in $\delta\theta_A(\mathbf{r})$. This means that to quadratic order the θ_A fluctuations of the hexagon do not interact with the rest of the lattice. It is these local excitations that produce the flat mode. Note that even classically, the energy of this distortion is not zero if higher orders in $\delta\theta_A$ are included. This is analogous to the flat mode in the $\mathbf{q}=0$ structure of the isotropic *kagomé* antiferromagnet, where once again, the mode is flat only to harmonic order.[35]

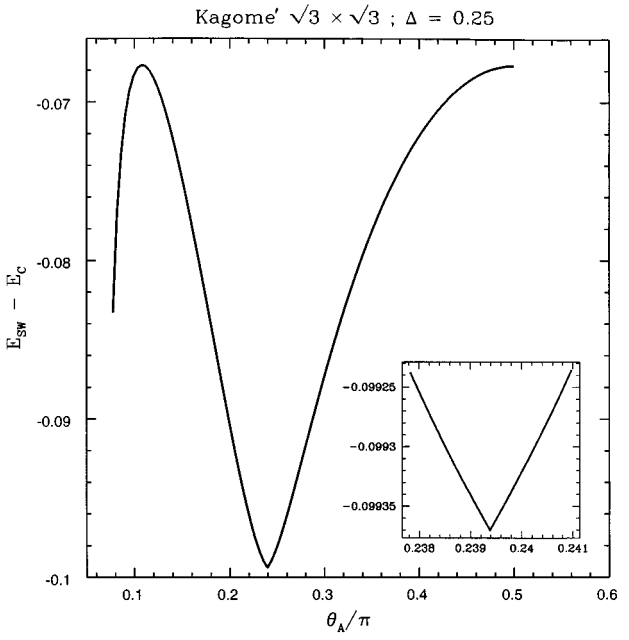

FIG. 22. Quantum energy correction versus θ_A for the *kagomé* *R*3 structure. Once again the leading-order potential has a linear cusp.

Consider this degeneracy mode in the presence of a small field. It is easy to show that the field energy (per nine site unit cell) near the optimal angles is

$$\delta E_{\text{field}}=\frac{3}{2}\,hS^2\,\frac{(2-\Delta)^2}{(1-\Delta)}\cos\theta_A(\delta\theta)^2. \tag{37}$$

We do not need to consider the bond energies of the spins to this order for the following reasons:

(i) One can decompose the deviation from the optimal θ_A, θ_B, θ_C into $\delta\theta_B=\delta\theta_{BA}+\delta\theta_B'$, and $\delta\theta_C=\delta\theta_{CA}+\delta\theta_C'$, where the first part represents the change in θ_B and θ_C along the degeneracy direction, due to the change in θ_A, and the primed part corresponds to a change orthogonal to the degeneracy direction.

(ii) The optimal $\delta\theta_B'$, $\delta\theta_C'$ in the presence of the field are of order h. This is because the bond energy is quadratic in $\delta\theta_B'$, $\delta\theta_C'$ while the field energy is linear in these quantities. Therefore, the energy difference due to the bonds will be of order h^2, which can be neglected in comparison to the order h field energy at small fields.

(iii) There is no bond energy associated with a change along $\delta\theta_A$.

The local ϕ mode conjugate to this θ_A mode is $[(1/2)\delta\phi, -(1/2)\delta\phi,0]$. The ''potential'' energy (per nine-site unit cell) of this mode can be calculated from the classical Hamiltonian exactly as in the triangular lattice case, and is

$$U=\frac{3}{2}\,S^2\Delta\phi^2\sin^2\theta_A^*\left(2+\frac{\sin\theta_C^*}{\sin\theta_A^*}\right). \tag{38}$$

The Berry phase term for this unit cell, $3S\,\sin\theta_A^*\delta\theta(\partial\phi^0/\partial\tau)$, allows us to identify $Q=3S\,\sin\theta_A^*\phi^0$ as the coordinate, and $P=\delta\theta$ as its conjugate momentum. Then

$$\omega(S,h,\Delta)=\tilde{\omega}(\Delta)S\sqrt{h},$$
$$\tilde{\omega}(\Delta)=\sqrt{\left(2+\frac{\sin\theta_C^*}{\sin\theta_A^*}\right)\frac{(2-\Delta)^2}{(1-\Delta)}\,\Delta\,\cos\theta_A^*}. \tag{39}$$

This gap goes to zero as $\sqrt{h}$ in the limit $h\to 0$, and the mode becomes gapless in addition to being flat.

So far we have used the field to stiffen the degeneracy mode. Now consider the effect of quantum fluctuations at $h=0$. We can find the effective potential to lowest leading order by computing the ground-state energy for various θ_A in SWT. This is plotted for $\Delta=0.25$ in Fig. 22. We assume that the mode will remain dispersionless, and therefore local, even when lifted from zero energy by quantum fluctuations. This assumption allows us to extract an effective Hamiltonian for each local degeneracy mode, which has been written down in Eq. (35), where we identify the *momentum* as

$P=3S\ \sin\theta_A^*\phi^0$ and the conjugate *coordinate* as $Q=\delta\theta$, and where the numerical value of λ is obtained from the figure (for $\Delta=0.25$):

$$M^{-1}=0.1944,$$
$$\lambda=0.025S. \tag{40}$$

We use a Gaussian trial wave function to obtain the approximate ground-state energy of this Hamiltonian, yielding

$$\omega_0\approx\left(\frac{27\lambda^2M^{-1}}{128\pi}\right)^{1/3}\approx 0.02S^{2/3}. \tag{41}$$

Of course, we expect this mode to disperse, but the calculation of the dispersion[43,44] is much harder than the one presented here, and will be pursued in future work.

III. EFFECT OF QUANTUM FLUCTUATIONS ON ORDER PARAMETERS

One of the motivations for this work has been to see if quantum fluctuations can disorder the system, creating a spin liquid, which would correspond to a ordinary liquid (with nonzero viscosity) for the bosons. To leading order in SWT, one can compute the average values of the spins as

$$\langle\mathbf{S}_i\rangle=(\langle a_i^\dagger a_i\rangle-S)\hat{\Omega}_{\rm MF}. \tag{42}$$

The calculation sketched out in Sec. II also produces the explicit Bogoliubov transformation, which can then be used to find the expectation values of bilinears. More explicitly, in terms of the matrix T which implements the transformation

$$\langle e_i^\dagger(\mathbf{k})e_j(\mathbf{k})\rangle=\sum_{\alpha=K+1}^{2K}T_{\alpha i}^\dagger(\mathbf{k})T_{j\alpha}(\mathbf{k}), \tag{43}$$

where it is understood that i and j run from 1 to K (the number of sublattices), while α runs from $K+1$ to $2K$, the rank of T. Let us now turn to the different cases.

A. Triangular lattice

Figure 3 shows a plot of the classical and quantum-corrected total S^z and total S^x, for $h=0$. It is clear that the quantum-corrected value of the magnetization is very close to zero, independent of Δ. Exact diagonalizations of finite clusters for the anisotropic antiferromagnetic case $\Delta<0$ (Ref. 45) suggest strongly that this is an exact statement. That is, the exact ground state at $h=0$ has zero longitudinal magnetization M_z. An interesting fact about the triangular lattice allows us to map the $\Delta>0$ problem (our model) to the $\Delta<0$ model, which is the anisotropic antiferromagnet solved in SWT by KMFF. For very small Δ one can work to linear order in Δ, which means that one is working within the set of antiferromagnetic Ising model ground states. For nearest-neighbor spin flips, the Marshall sign property is obeyed by the wave functions, arising from a partition of the set of ground states into disjoint even and odd states.[46] This means that for very small Δ there is evidence that the boson system would be exactly half-filled in the true ground state. However, to any higher order in Δ, or numerically for Δ not so small, the two models have no simple relationship with each other since the triangular lattice is not bipartite.

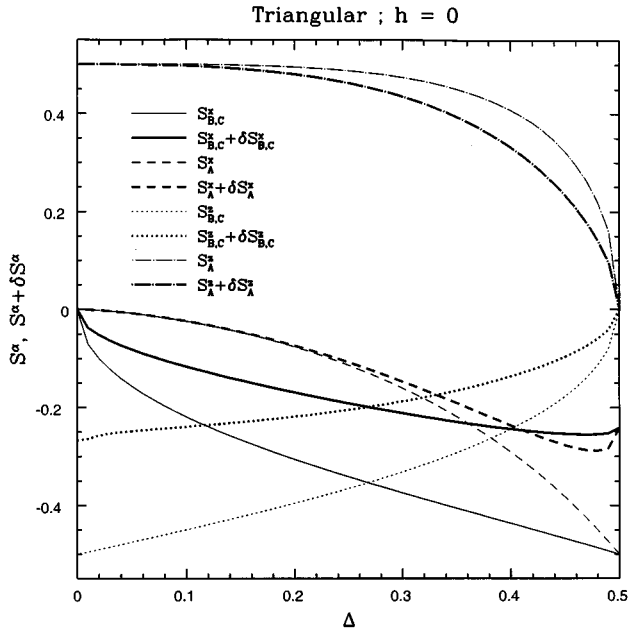

FIG. 23. Quantum fluctuation corrections to the magnitudes of the spins on the A and C sublattices as a function of Δ at $h=0$ for the triangular lattice.

Although total S^x decreases as Δ decreases, it seems that superfluid order persists all the way, vanishing only when $\Delta=0$. In Fig. 23 we plot the quantum fluctuation corrections to the magnitudes of the spins on the three sublattices (since $\theta_B=\theta_C$ we plot only two values). As $\Delta\to 0$ the A sublattice remains stiff, while the B and C sublattice spins get reduced to about half their classical value (for $S=1/2$). Thus, supersolid order on the triangular lattice survives quantum fluctuations at the spin-wave level.

Let us now turn to Fig. 24, which shows the classical and quantum order parameters as a function of Δ for $h=3$. For $\Delta<1/2$ it is clear that though there are quantum fluctuation corrections to each of the spins, the total S_z is not corrected, thus leaving the filling exactly 2/3. For $\Delta>1/2$, there are fluctuation corrections which do not affect the nature of the phase. Once again, we will concentrate on the lower energy $\sqrt{3}\times\sqrt{3}$ structure on the *kagomé* lattice, leaving an analysis of the $\mathbf{q}=0$ structure to future work.

B. kagomé 9 sublattice structure

Figure 5 presents the naive results for the occupation numbers of the different sublattices in SWT for the $\sqrt{3}\times\sqrt{3}$ structure at $\Delta=0.25$ as a function of h. Notice that as $h\to 0$ the fluctuation corrections diverge. This is a consequence of the flat mode, whose energy goes to zero as $h\to 0$. In reality, as we have seen in the previous section, the energy flat mode will be lifted in higher orders of SWT. While a quantitatively accurate analysis requires the computation of the dispersion of this degeneracy mode, we can make a rough estimate of the fluctuation corrections to the sublattice spins by assuming that the mode remains flat at the value ω_1 calculated in Sec. II C 2.

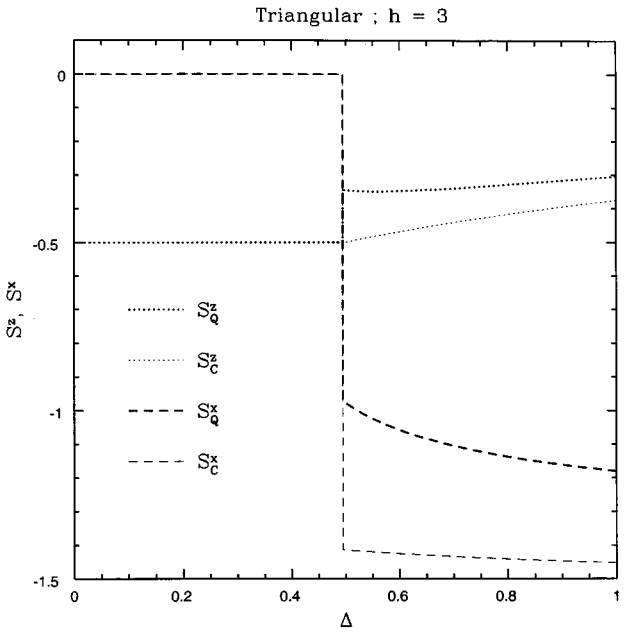

FIG. 24. Classical and quantum values of S_z and S_x for the triangular lattice at $h=3$ as a function of Δ. Note that for $\Delta<1/2$ we are in the MI phase, and the total magnetization is uncorrected from its mean-field value of 2/3.

We need to determine the reduction in the magnitude of each sublattice spin due to quantum fluctuations. In terms of the equilibrium position θ^* and the deviations from equilibrium $\delta\theta$ and $\delta\phi$ we can write the magnitude of the spin as

$$|\langle \mathbf{S}\rangle| = S\left(1-\frac{1}{2}(\delta\theta)^2-\frac{1}{2}\sin^2\theta^*\phi^2\right)=\left(1-\frac{P^2}{2}-\frac{Q^2}{18S^2}\right), \tag{44}$$

where we have once again used $P=3S\sin\theta_A^*\phi^0$ and $Q=\theta_A$, and assumed a nondispersing degeneracy mode.

We know from the harmonic oscillator that

$$\langle P^2\rangle_0=\frac{\omega}{2M^{-1}},$$
$$\langle Q^2\rangle_0=\frac{\omega}{2K}, \tag{45}$$

and in the case $h\neq 0$, we find

$$|\langle \mathbf{S}\rangle| = S-\frac{1}{12S\sqrt{h}}\left(\sqrt{\frac{\Delta(2+\sin\theta_C^*/\sin\theta_A^*)}{\cos\theta_A^*[(2-\Delta)^2/1-\Delta]}}+\frac{h}{2}\sqrt{\frac{\cos\theta_A^*[(2-\Delta)^2/1-\Delta]}{\Delta(2+\sin\theta_A^*/\sin\theta_A^*)}}\right). \tag{46}$$

Clearly there is a divergence as $h\to 0$, which is seen in Fig. 5. Of course, there will also be a contribution independent of h due to the other modes not associated with the degeneracy.

Now consider the case $h=0$. As shown in the previous section, the flat mode will be lifted from zero energy by quantum fluctuations and acquire an energy of order $S^{2/3}$. We will assume that the mode does not disperse (even though it will, weakly) in order to estimate the quantum fluctuations in the sublattice spins. We will also assume that none of the matrix elements change substantially. Thus the energy of the mode is the only significant factor. This means that we can estimate the contribution to the fluctuation correction to the spins by applying a field h_Q such that the field-induced energy is the same as the energy induced by quantum fluctuations:

$$h_Q\approx\frac{\lambda^2}{\tilde{\omega}^2}S^{-2/3}. \tag{47}$$

Numerically, we find for $\Delta=0.25$ that $h_Q=0.000\,57$. This implies boson occupations of $n_A=n_B=1.66$, and $n_C=0.04$. Since the boson occupations are larger than the value $S=1/2$, we find the fluctuations to be larger than the mean-field value of the spin. Thus, despite the lifting of the flat mode due to quantum fluctuations, we find that fluctuations may be large enough to disorder the mean-field ordering on the A and B sublattices. However, it is not certain that large fluctuations imply disorder. Furthermore, it is difficult to understand how the C sublattice could remain stiff and ordered if the other two lattices are disordered. Strictly speaking, what this result tells us is that we have reached the limitations of spin-wave theory.

CONCLUSIONS AND OPEN QUESTIONS

We have found a broad region of parameter space where supersolid order is stable to leading order in mean-field theory. The inclusion of spin-wave corrections modifies this picture differently for the triangular and *kagomé* lattices. The supersolid is quite robust on the triangular lattice. Our interpretation of the supersolid corresponds with the ideas of Andreev and Lifshitz,[1] with hopping vacancies undergoing Bose condensation. The role of lattice frustration is to prevent all the particles from condensing into a solid.

We have also come across a general (though nonrigorous) argument which limits the search for the true ground state in a system with ground-state degeneracy: Look for the points at which global conserved quantities commute in the Poisson bracket sense with the generators of motion on the degeneracy subspace.

On the *kagomé* lattice we find the $\sqrt{3}\times\sqrt{3}$ structure to be more stable than the $\mathbf{q}=0$ structure at all parameter values. Fluctuations seem much stronger here, and may even be able to destroy the long-range order assumed in mean-field theory. This is a fertile region for numerical and experimental work.

To what experimental systems might these considerations be applicable? One might be able to construct an array of Josephson junctions[47] which satisfy the conditions necessary for the existence of a supersolid. This means that the charging energy of each grain should be very high, and the nearest-neighbor charging energy should be higher than the Josephson coupling between the neighboring grains. Furthermore, only pair hopping should be relevant, which implies temperatures low compared to the bulk superconducting T_c. Of course, since this is a two-dimensional system, the Bose condensate disappears for $T\neq 0$, but power-law ODLRO is expected to remain.

Another experimental system to which these results might be relevant is ^{4}He on graphite. A variety of orderings and transitions are known to occur as a function of temperature and coverage.[48] Also, steps in the superfluid density have been seen as a function of coverage (for multiple layers) for ^{4}He on graphite,[49] and have been interpreted as resulting from correlation effects.[50]

As it stands, this work is *not* applicable to the question of supersolidity in ^{4}He on a smooth substrate. In order to approach the continuum one would have to consider very low densities on the lattice, as well as long-range interactions (see Ref. 15 for an example of a continuum approach). We close with a number of important open questions.

SWT seems sufficient for the triangular lattice, but not for the *kagomé* lattice. A formalism that can consider ordered and disordered states in a unified manner is necessary, perhaps a variant of the large-N approaches.[51,36] Second, even for the triangular lattice, the question of vortices in the ground state is open. The spin-wave ground state has vortices, but they occur in nearest-neighbor pairs. A fruitful way to incorporate vortices might be to consider the effective theory of the gapless modes only, and include their interaction with vortices in a semiclassical manner.

The original picture of Ref. 20 has been confirmed by a strong-coupling expansion.[10] Strong-coupling expansions and variational approaches[52,53] are complimentary to the spin-wave expansion, and it would be interesting to investigate our model by these approaches.

The effects of nonzero temperature on systems with ground-state degeneracy can be very nontrivial. In particular, quantum and thermal ground-state selection effects may compete to produce a sequence of phases and transitions as the temperature is raised.[29] Clearly, thermal effects have to be elucidated before our results can be directly applied to an experimental situation. Finally, it is intriguing to harken back to the question raised by Anderson and Fazekas[24] and ask whether it is possible for a liquid state to be stable at zero temperature.

ACKNOWLEDGMENTS

It is a pleasure to thank John Clarke, Subir Sachdev, Steve Kivelson, Dung-hai Lee, Shoucheng Zhang, Zlatko Tesanovic, and Dan Rokhsar for valuable discussions. We are especially grateful to Chris Henley for detailed comments on draft versions and enlightening discussions. This research was supported in part by NSF Grant No. DMR-9311949 (G.M.). G.M. and D.P.A. are also grateful for the hospitality of the Technion at Haifa, where this work was initiated.

APPENDIX: CONTINUOUS DEGENERACY NOT ARISING FROM A SYMMETRY

Consider a Hamiltonian function $\mathcal{H}(\mathbf{x})$, where

$$\mathbf{x}=(p_1,p_2,\ldots,p_N,q_1,q_2,\ldots,q_N) \tag{A1}$$

is the vector of (dimensionless) coordinates and momenta. What does it mean that the ground state is continuously degenerate? Clearly, there must exist a one-parameter family of ground states, i.e.,

$$\left(\frac{\partial\mathcal{H}}{\partial x_\mu}\right)_{\mathbf{X}(\lambda)}=0 \tag{A2}$$

for all $\mu=1,\ldots,2N$, where λ parametrizes the degeneracy submanifold, a curve in phase space defined by $\mathbf{X}(\lambda)$. The degeneracy submanifold is one dimensional in this example. Differentiating with respect to λ gives

$$\sum_{\nu=1}^{2N}\left(\frac{\partial^2\mathcal{H}}{\partial x_\mu\partial x_\nu}\right)_{\mathbf{X}(\lambda)}\frac{\partial X_\nu(\lambda)}{\partial\lambda}=0, \tag{A3}$$

i.e., the vector $\partial X_\nu/\partial\lambda$ is a null eigenvector of the Hessian matrix evaluated at the point $\mathbf{X}(\lambda)$.

As an example, consider the function

$$\mathcal{H}(r,\phi)=\frac{1}{4}(r^2-1)^2(a+b\,\cos\phi), \tag{A4}$$

whose minimum is at $r=1$ independent of ϕ. Note that ϕ is not cyclic in $\mathcal{H}$, and its conjugate momentum (say r^2, by definition) is not conserved as Noether's theorem does not apply. Nonetheless, there is a one-parameter family of ground states, parametrized by ϕ. The Hessian matrix, evaluated at $r=1$, is

$$H=\begin{pmatrix}2(a+b\,\cos\phi) & 0\\ 0 & 0\end{pmatrix} \tag{A5}$$

and the vector $(\partial/\partial\phi)\binom{r^2}{\phi}=\binom{0}{1}$ is a null eigenvector.

Now consider the Gaussian fluctuations about the ground state. We are interested in the partition function $Z=\int\mathcal{D}[p,q]e^{-\mathcal{A}}$, which is obtained from the action functional

$$\mathcal{A}=\int_0^{\beta\hbar}d\tau\left(i\hbar\sum_i q_i\frac{\partial p_i}{\partial\tau}+\mathcal{H}(\mathbf{p},\mathbf{q})\right), \tag{A6}$$

where $i=1,\ldots,N$. We expand about one of the ground states, writing $p_i=P_i+\delta p_i$, $q_i=Q_i+\delta q_i$, and, using summation convention,

$$\mathcal{H}=\frac{\hbar}{2}\,\delta p_i T_{ij}\delta p_j+\frac{\hbar}{2}\,\delta p_i R_{ij}\delta q_j+\frac{\hbar}{2}\,\delta q_i R^t_{ij}\delta p_j+\frac{\hbar}{2}\,\delta q_i V_{ij}\delta q_j \tag{A7}$$

with

$$T_{ij}=\frac{1}{\hbar}\left(\frac{\partial^2\mathcal{H}}{\partial p_i\partial p_j}\right)_{\mathbf{P},\mathbf{Q}},\quad R_{ij}=\frac{1}{\hbar}\left(\frac{\partial^2\mathcal{H}}{\partial p_i\partial q_j}\right)_{\mathbf{P},\mathbf{Q}},\quad V_{ij}=\frac{1}{\hbar}\left(\frac{\partial^2\mathcal{H}}{\partial q_i\partial q_j}\right)_{\mathbf{P},\mathbf{Q}}, \tag{A8}$$

and R^t is the transpose of R. Thus, the integrand of $\mathcal{A}$ is given by $(\hbar/2)\,\delta x_\mu(H_{\mu\nu}+iJ_{\mu\nu}\partial_\tau)\,\delta x_\nu$, where

$$H=\begin{pmatrix}T & R\\ R^t & V\end{pmatrix} \tag{A9}$$

and

$$J=\begin{pmatrix} 0_{N\times N} & 1_{N\times N} \\ -1_{N\times N} & 0_{N\times N} \end{pmatrix}. \tag{A10}$$

The matrix H is brought to diagonal form by the basis change S:

$$S^\dagger HS=\begin{pmatrix} \Omega^+ & 0 \\ 0 & \Omega^- \end{pmatrix}, \tag{A11}$$

where $\Omega^\pm=\mathrm{diag}(\omega_1^\pm,\ldots,\omega_N^\pm)$ is a diagonal matrix, and $S^\dagger JS=J$ preserves the symplectic structure (commutation relations). Note that the diagonalized Hamiltonian is $(1/2)(p^t\Omega^+p+q^t\Omega^-q)$ rather than, say $(1/2)(p^tp+q^t\Omega^2q)$. The two are, of course, related by a canonical transformation, provided the $\omega_k^\pm$ are nonzero.) The eigenvectors come in pairs $|\psi_k^\pm\rangle$ which satisfy

$$JH|\psi_k^+\rangle=-\omega_k^+|\psi_k^-\rangle,$$

$$JH|\psi_k^-\rangle=+\omega_k^-|\psi_k^+\rangle,$$

as well as the orthonormalization condition

$$\langle\psi_k^+|J|\psi_l^+\rangle=\langle\psi_k^-|J|\psi_l^-\rangle=0,$$

$$-\langle\psi_k^-|J|\psi_l^+\rangle=\langle\psi_k^+|J|\psi_l^-\rangle=\delta_{kl},$$

where $k,l=1,\ldots,N$. The N energy eigenvalues are then given by $\mathbf{e}_k=\hbar\sqrt{\omega_k^+\omega_k^-}$.

Now consider the case where the degeneracy subspace is two dimensional, parametrized by the coordinates (λ,ξ). In our spin-wave theory, we have that $q_i=\phi_i$ and $p_i=S(1-\cos\theta_i)$, and the λ invariance is realized as some relation among the colatitutes $\Theta_i(\lambda)$ along the ground-state submanifold, while the ξ invariance is simply expressed as $\Phi_i(\xi)=\Phi_i(0)+\xi$. The matrix H (and hence JH) has two known null right eigenvectors—call them $|N_1\rangle$ and $|N_2\rangle$—corresponding, respectively, to the λ and ξ invariances. We have that

$$|N_1\rangle=\begin{pmatrix} \dfrac{\partial P_i}{\partial\lambda} \\ \dfrac{\partial Q_i}{\partial\lambda} \end{pmatrix}=\begin{pmatrix} S\,\sin\Theta_i\,\dfrac{\partial\Theta_i}{\partial\lambda} \\ 0_N \end{pmatrix} \tag{A12}$$

and

$$|N_2\rangle=\begin{pmatrix} \dfrac{\partial P_i}{\partial\xi} \\ \dfrac{\partial Q_i}{\partial\xi} \end{pmatrix}=\begin{pmatrix} 0_N \\ 1_N \end{pmatrix}. \tag{A13}$$

Note that the $|N_2\rangle$ eigenvector contains a 1 in each of its lower N entries. When we compute the overlap $\langle N_2|J|N_1\rangle$, we obtain

$$\langle N_2|J|N_1\rangle=-\sum_{i=1}^{N} S\,\sin\Theta_i\,\frac{\partial\Theta_i}{\partial\lambda}=\frac{\partial M^z}{\partial\lambda}, \tag{A14}$$

where M^z is the total $\hat{z}$ component of the magnetization: $M^z\equiv\sum_{i=1}^{N}S\cos\Theta_i$. Unless the magnetization M_z is extremized with respect to λ, there is a finite overlap, and by appropriate normalization one can choose $|N_1\rangle$ and $|N_2\rangle$ to be a $|\psi^\pm\rangle$ pair. When the magnetization is extremized, however, the overlap is zero which means that these two null right eigenvectors belong to separate pairs, and there are at least *two* zero modes.

Therefore, *the two modes are independent only when $\partial M^z/\partial\lambda=0$, that is to say, when the magnetization M^z is extremized*. In the general case both the conserved quantity and the generator of motion along the degeneracy subspace may have components along both p and q subspaces. It is then easy to see that the two vectors will have zero overlap only if the conserved quantity commutes (in the Poisson bracket sense) with the generator of motion along the degeneracy subspace.

*Permanent address: Department of Physics, Boston University, Boston, MA.

[1] A. F. Andreev and I. M. Lifshitz, Sov. Phys. JETP **29**, 1107 (1969).

[2] M. W. Meisel, Physica B **178**, 121 (1992).

[3] G. A. Lengua and J. M. Goodkind, J. Low Temp. Phys. **79**, 251 (1990).

[4] G. V. Chester, Phys. Rev. A **2**, 256 (1970).

[5] A. J. Leggett, Phys. Rev. Lett. **25**, 1543 (1970).

[6] C. Bruder, R. Fazio, and G. Schön, Phys. Rev. B **47**, 342 (1993).

[7] A. van Otterlo, K.-H. Wagenblast, R. Fazio, and G. Schön, Phys. Rev. B **48**, 3316 (1993).

[8] A. van Otterlo, K.-H. Wagenblast, R. Baltin, C. Bruder, R. Fazio, and G. Schön, Phys. Rev. B **52**, 16 176 (1995).

[9] E. Roddick and D. Stroud, Phys. Rev. B **48**, 16 600 (1993).

[10] J. K. Freericks and H. Monien, Europhys. Lett. **26**, 545 (1994).

[11] P. Niyaz, R. T. Scalettar, C. Y. Fong, and G. G. Batrouni, Phys. Rev. B **44**, 7143 (1991).

[12] P. Niyaz, R. T. Scalettar, C. Y. Fong, and G. G. Batrouni, Phys. Rev. B **50**, 362 (1994).

[13] A. P. Kampf and G. T. Zimanyi, Phys. Rev. B **47**, 279 (1993).

[14] R. T. Scalettar, G. G. Batrouni, A. P. Kampf, and G. T. Zimanyi, Phys. Rev. B **51**, 8467 (1995).

[15] Y. Pomeau and S. Rica, Phys. Rev. Lett. **72**, 2426 (1994).

[16] The correspondence between the world lines of two-dimensional bosons and vortex lines in three-dimensional superconductors, derived in M. P. A. Fisher and D.-H. Lee, Phys. Rev. B **39**, 2756 (1989), and D. R. Nelson and H. S. Seung, *ibid*. **39**, 9153 (1989), provides another paradigm for supersolid behavior, in which defects in a flux-line lattice condense to form a supersolid state which might intervene between the vortex line crystal and entangled line liquid phases. See, e.g., E. Frey, D. R. Nelson, and D. S. Fisher, Phys. Rev. B **49**, 9723 (1994).

[17] S. Doniach, Phys. Rev. B **24**, 5063 (1981).

[18] H. Matsuda and T. Tsuneto, Prog. Theor. Phys. **46**, 411 (1970).

[19] K.-S. Liu and M. E. Fisher, J. Low Temp. Phys. **10**, 655 (1973).

[20] M. P. Fisher, P. B. Weichman, G. Grinstein, and D. S. Fisher, Phys. Rev. B **40**, 546 (1989).

[21] M. Wallin, E. S. Sorensen, S. M. Girvin, and A. P. Young, Phys. Rev. B **49**, 12 115 (1994).

[22] See, for example, A. Auerbach, *Correlated Electrons and Quantum Magnetism* (Springer-Verlag, New York, 1994), and references therein.

[23] P. W. Anderson, Mater. Res. Bull. **8**, 153 (1973).
[24] P. Fazekas and P. W. Anderson, Philos. Mag. **30**, 423 (1974).
[25] E. F. Shender, Sov. Phys. JETP **56**, 178 (1982).
[26] C. L. Henley, Phys. Rev. Lett. **62**, 2506 (1989).
[27] B. Kleine, E. Müller-Hartmann, K. Frahm, and P. Fazekas, Z. Phys. B **87**, 103 (1992).
[28] A. V. Chubukov and D. I. Golosov, J. Phys. Condens. Matter **3**, 69 (1991).
[29] Q. Sheng and C. L. Henley, J. Phys. Condens. Matter **4**, 2937 (1992).
[30] S. Miyashita and H. Kawamura, J. Phys. Soc. Jpn. **54**, 3385 (1985).
[31] V. Elser, Phys. Rev. Lett. **62**, 2405 (1989).
[32] C. Zeng and V. Elser, Phys. Rev. B **42**, 8436 (1990).
[33] C. Zeng and V. Elser, Phys. Rev. B **51**, 8318 (1995).
[34] J. B. Marston and C. Zeng, J. Appl. Phys. **69**, 5962 (1991).
[35] A. B. Harris, C. Kallin, and A. J. Berlinsky, Phys. Rev. B **45**, 2899 (1992).
[36] S. Sachdev, Phys. Rev. B **45**, 12 377 (1992).
[37] P. Chandra and P. Coleman, Phys. Rev. Lett. **66**, 100 (1991).
[38] P. Chandra, P. Coleman, and I. Ritchey, Int. J. Mod. Phys. B **5**, 17 (1991).
[39] We are indebted to Steve Kivelson for making us aware of the calculation of the gap of the degeneracy mode in Ref. 25.
[40] We are indebted to Chris Henley for making us aware of weaknesses in our original argument.
[41] J. van Delft and C. L. Henley, Phys. Rev. B **48**, 965 (1993).
[42] I. Ritchey, P. Chandra, and P. Coleman, Phys. Rev. B **47**, 15 342 (1993).
[43] A. V. Chubukov, Phys. Rev. Lett. **69**, 832 (1992).
[44] H. Asakawa and M. Suzuki, Int. J. Mod. Phys. B **9**, 933 (1995).
[45] B. Kleine, P. Fazekas, and E. Müller-Hartmann, Z. Phys. B **86**, 405 (1992).
[46] H. W. J. Blöte and H. J. Hillhorst, J. Phys. A **15**, L631 (1982).
[47] L. J. Geerligs, M. Peters, L. E. M. de Groot, A. Verbruggen, and J. E. Mooij, Phys. Rev. Lett. **63**, 326 (1989).
[48] M. Bretz, J. G. Dash, D. C. Hickernell, E. O. McLean, and O. E. Vilches, Phys. Rev. B **8**, 1589 (1973).
[49] P. A. Crowell and J. D. Reppy, Phys. Rev. Lett. **70**, 3291 (1993).
[50] G. T. Zimanyi, P. A. Crowell, R. T. Scalettar, and G. G. Batrouni, Phys. Rev. B **50**, 6515 (1994).
[51] D. P. Arovas and A. Auerbach, Phys. Rev. Lett. **61**, 617 (1988); Phys. Rev. B **38**, 316 (1988).
[52] D. S. Rokhsar and B. G. Kotliar, Phys. Rev. B **44**, 10 328 (1991).
[53] W. Krauth, M. Caffarel, and J.-P. Bouchard, Phys. Rev. B **45**, 3137 (1992).